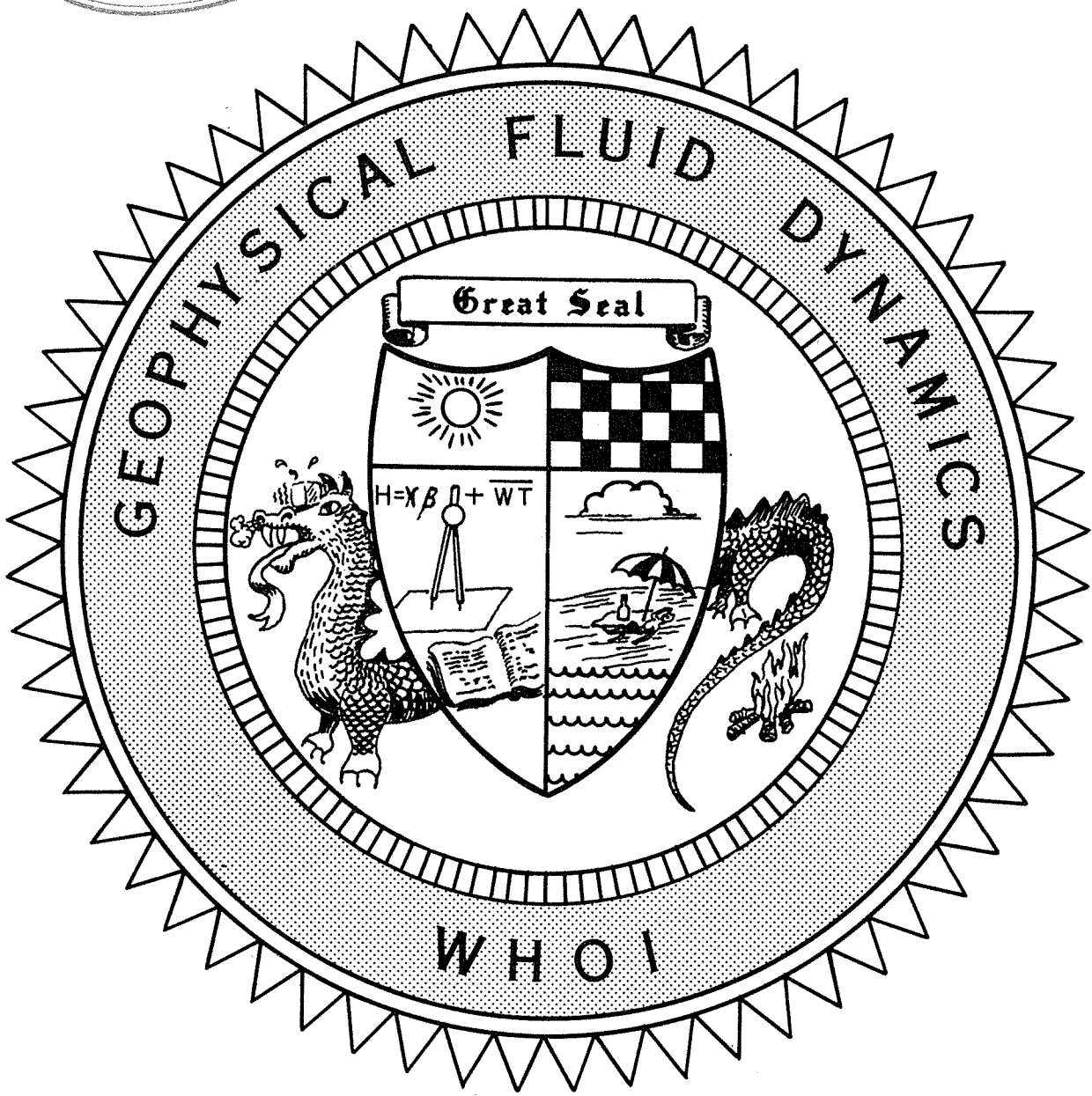


REF. 62-33  
**1962**

*Copy 2*

WHOI  
DOCUMENT  
COLLECTION



STUDENT LECTURES

Notes on the 1962  
Summer Study Program  
in  
GEOPHYSICAL FLUID DYNAMICS  
at  
The WOODS HOLE OCEANOGRAPHIC INSTITUTION



Reference No. 62-33

#### LIST OF PARTICIPANTS

Prof. Arnt Eliassen, University of Oslo, Blindern, Norway  
Dr. George B. Field, Princeton Observatory, Princeton, New Jersey  
Dr. Raymond Hide, Massachusetts Institute of Technology  
Dr. R. H. Kraichnan, Institute for Mathematical Sciences, New York  
Dr. Willem V.R. Malkus, University of Southern California at Los Angeles  
Dr. Leon Mestel, Trinity College, Cambridge University, England  
Dr. Eric Mollo-Christensen, Massachusetts Institute of Technology  
Dr. Derek Moore, Bristol University, Bristol, England  
Dr. Alan Robinson, Harvard University  
Dr. Claus Rooth, Woods Hole Oceanographic Institution  
Dr. Edward A. Spiegel, Institute for Mathematical Sciences, New York  
Dr. Melvin Stern, Woods Hole Oceanographic Institution  
Prof. Henry Stommel, Harvard University  
Dr. Alar Toomre, Massachusetts Institute of Technology  
Dr. George Veronis, Woods Hole Oceanographic Institution

#### STUDENT FELLOWS

Peter Bryant, Emmanuel College, Cambridge, England  
James Holton, Massachusetts Institute of Technology  
Joseph Pedlosky, Massachusetts Institute of Technology  
Hans Thomas Rossby, Royal Technical University, Stockholm, Sweden  
(now M.I.T.)  
Pierre Souffrin, Institut d'Astrophysique, Paris, France  
Roger T. Williams, University of Southern California at Los Angeles

### Acknowledgment

This volume contains the manuscripts of the student research lectures. We should like to thank the National Science Foundation for the financial support which made this year's program of study and research possible.

In addition we owe our gratitude to Dr. Leon Mestel of Cambridge University for his lecture series "Topics in Astrophysical Hydrodynamics", and to Dr. Robert Kraichnan of New York University for his series "Topics in Turbulence Theory".

Mrs. Mary Thayer is to be thanked again for her conscientious preparation of this volume from the manuscripts. Although each author is responsible for his contribution, the time factor has prevented them from checking the printed version.

Melvin Stern.

## Table of Contents

Wind Flow over Water Waves  
by Peter J. Bryant.

An Attempt to Simulate the Cromwell Current in the Laboratory  
by James R. Holton.

Baroclinic Instability in Two Layer Systems  
by Joseph Pedlosky.

Experiments in Thermal Convection  
by Hans Thomas Rossby.

On the Problem of Finite Amplitude Convection  
by P. Souffrin.

Finite Amplitude Evolution of Large Scale Atmospheric Disturbance  
by R. T. Williams.

Wind Flow over Water Waves

by

Peter J. Bryant

# Wind Flow over Water Waves

by

Peter J. Bryant

## 1. Introduction

When a turbulent wind begins to blow over an infinite horizontal water surface, the initial disturbances in the water are due to the turbulent stress fluctuations at the water surface. However, as soon as a wave pattern is generated, there will be a coupling between the motion of the water surface and the air motion, modifying the surface stress pattern. This investigation is into the nature of this coupling. A complete review of the subject of wind generation of water waves has been made by Phillips (1962).

It has been the custom to assume that the air motion is laminar and that the turbulent fluctuations contribute only to the shape of the mean velocity profile. This assumption is examined, and a form of justification attempted.

When this assumption has been made, the air motion is described by the Orr-Sommerfeld equation. In order to derive a qualitative solution, the inviscid motion of separate parcels of fluid is examined, and deductions are made from the solutions obtained concerning the real state, in the manner suggested by Lighthill (1962).

## 2. Equations for the air motion

The water surface is assumed to be of the form

$$\eta = a \sin k(x-ct)$$

where  $a$  is a slowly varying function of time. This can be interpreted as being one Fourier component of the real surface, because interactions between these Fourier components are non-linear, and in this investigation non-linear interactions are being neglected. The  $y$ -axis is chosen to be vertically upwards, with origin in the mean free surface, and the motion is assumed to be two dimensional. This is not strictly true for the turbulent fluctuations, but the fluctuations appearing here may be considered as the  $z$ -means of the actual fluctuations.

The equations to be considered are therefore

$$\begin{aligned} \frac{\partial u}{\partial t} + \frac{\partial}{\partial x}(u^2) + \frac{\partial}{\partial y}(uv) &= -\frac{1}{\rho} \frac{\partial p}{\partial x} + \nu \nabla^2 u \\ \frac{\partial v}{\partial t} + \frac{\partial}{\partial x}(uv) + \frac{\partial}{\partial y}(v^2) &= -\frac{1}{\rho} \frac{\partial p}{\partial y} + \nu \nabla^2 v \\ \frac{\partial u}{\partial x} + \frac{\partial v}{\partial y} &= 0 \end{aligned} \quad (2.1)$$

The mean of these equations will be taken in two ways.

If  $f(x,y,t)$  represents one of the functions appearing, define

$$\bar{f}^x = \lim_{X \rightarrow \infty} \frac{1}{2X} \int_{-X}^{+X} f dx \quad (2.2)$$

and

$$\bar{f}^t = \frac{1}{T} \int_0^T f dt$$

where  $\frac{1}{a} \frac{da}{dt} \ll \frac{1}{T} \ll \pi$ ,

$\pi$  being the wave frequency. To be more precise,  $T$  can be chosen to be an integral number of periods, satisfying the relation. It has been assumed here that the development time of the amplitude is very much greater than the wave period, and physically this can be seen to be true, provided that the wind is not too strong.

The origin in  $x$  is chosen to be travelling with the wave velocity  $c$ , so as to reduce the wave motion to a near steady state.

Let

$$\begin{aligned} u(x,y,t) &= U(y) - c + u_1(x,y) + u_2(x,y,t) \\ v(x,y,t) &= v_1(x,y) + v_2(x,y,t) \\ p(x,y,t) &= P(y) + p_1(x,y) + p_2(x,y,t) \end{aligned} \quad (2.3)$$

where, using  $f$  as above,

$$\begin{aligned} \overline{f_2^x} &= \overline{f_2^t} = 0 & \text{ie } f_2 &= f - \overline{f^t} \\ \overline{f_1^x} &= 0 & \text{ie } f_1 &= \overline{f^t} - \overline{f^x} \end{aligned} \quad (2.4)$$

$f_1$  is that part of the air motion which is coupled with the water motion, and  $f_2$  is the random air motion.

If  $f, g$  are any two such functions, not necessarily different, then

$$\begin{aligned} \overline{f_1 g_2^t} &= 0 \\ \overline{f_2^t} &= \overline{f_2^x} \end{aligned} \quad (2.5)$$

the latter equality arising from the properties of homogeneity in the  $x$  direction and near stationarity for the random air motion.

Also  $\overline{f_1^2}^x$ ,  $\overline{f_2^2}^x$ ,  $\overline{f_2^2}^t$  are independent of  $x$ , and vary only slowly with  $t$ . (When there is no confusion, the meaned variable will not be indicated.)

The boundary conditions are taken to be

$$u_1, v_1, p_1 \rightarrow 0 \text{ as } y \rightarrow \infty \text{ and } u_2, v_2 = 0 \text{ on } y = 0,$$

Taking the means of equations (2.1) in the various ways, and carrying out integration, obtain

$$\begin{aligned} \overline{u_1 v_2}^x + \overline{u_2 v_1}^x &= 0 \\ \overline{v_1 v_2}^x &= 0 \end{aligned} \quad (2.6)$$

$$\overline{v_1^2} + \overline{v_2^2} = \frac{P_\infty}{\rho} - \frac{P(y)}{\rho} + \overline{v_2^2}_\infty \quad (2.7)$$

$$\frac{\partial}{\partial y} (\overline{u_1 v_1} + \overline{u_2 v_2}) = \nu \frac{\partial^2 U}{\partial y^2} \quad (2.8)$$

$$(U-c) \frac{\partial u_1}{\partial x} + v_1 \frac{\partial u_1}{\partial y} + \frac{\partial}{\partial x} (u_1^2) + \frac{\partial}{\partial y} (u_1 v_1 - \overline{u_1 v_1}) = -\frac{1}{\rho} \frac{\partial p_1}{\partial x} + \nu \nabla^2 u_1, \quad (2.9)$$

$$(U-c) \frac{\partial v_1}{\partial x} + \frac{\partial}{\partial x} (u_1 v_1) + \frac{\partial}{\partial y} (v_1^2 - \overline{v_1^2}) = -\frac{1}{\rho} \frac{\partial p_1}{\partial y} + \nu \nabla^2 v_1, \quad (2.10)$$

$$\frac{\partial u_1}{\partial x} + \frac{\partial v_1}{\partial y} = 0 \quad (2.11)$$

Equations (2.6) could probably have been assumed initially, but were not since they follow from the assumptions already made. Equation (2.7) gives the variation of the mean pressure, which here is the driving force of the system. Equation (2.8) will be integrated below, since it contains a singularity at the critical layer. Equations (2.9) (2.10) (2.11) with the non-linear terms

excluded, are the Orr-Sommerfeld equations, and are the justification for the assumption of laminar air motion, but with the mean velocity profile dependent on the total fluctuations.

### 3. Description of the air motion

The motion represented by the inviscid Orr-Sommerfeld equation (the Rayleigh equation) is now examined. The subscript 1 is omitted, and the origin of co-ordinates is fixed in space.

The frequency of oscillation of a parcel of air seen by an observer moving with the mean wind is  $k(U(y) - c)$ . Hence the vertical velocity,  $v$ , and the displacement,  $h$ , of this parcel are given by

$$v = v_0(y) \cos k(U-c)t \quad (3.1)$$

$$h = v_0(y) \frac{\sin k(U-c)t}{k(U-c)} \quad (3.2)$$

The equation of continuity shows that

$$u = U(y) - \frac{dv_0(y)}{dy} \frac{1}{k} \sin k(U-c)t - v_0(y) \frac{d\epsilon(y)}{dy} \frac{1}{k} \cos k(U-c)t \quad (3.3)$$

where  $\epsilon(y)$  is the phase and is defined by

$$k(U-c)t = k(x-ct) + \epsilon(y) \quad (3.4)$$

The vorticity  $\omega$  is

$$\begin{aligned} \omega &= \frac{\partial v}{\partial x} - \frac{\partial u}{\partial y} \\ &= - \frac{\partial U(y-h)}{\partial y} \end{aligned}$$

by the Kelvin Helmholtz conservation of vorticity,

$$\text{ie } \omega = -\frac{\partial u}{\partial y} + h \frac{\partial^2 u}{\partial y^2} \quad (3.5)$$

to the first order.

Taking the mean of the horizontal equation of motion, and using the equation of continuity

$$\frac{\partial \bar{u}}{\partial t} = -\frac{\partial}{\partial y} (\bar{u}v) = \bar{\omega}v \quad (3.6)$$

all these terms being of the second order.

$$\begin{aligned} \bar{\omega}v &= U''(y) \bar{h}v \\ &= U''(y) v_0^2(y) \frac{\sin 2k(U-c)t}{2k(U-c)} \\ &= U''(y) v_0^2(y) \frac{\pi \delta(y-y_c)}{2k U'(y_c)} \left( \begin{array}{l} y=y_c \\ \text{at } U=c \end{array} \right) \\ &= \frac{\pi}{2k} \frac{U''(y_c)}{U'(y_c)} v_0^2(y_c) \delta(y-y_c) \end{aligned} \quad (3.7)$$

where the relation used is

$$\frac{\sin zt}{z} = \lim_{t \rightarrow \infty} \frac{\sin zt}{z} = \pi \delta(z) \quad (3.8)$$

and  $\delta(z)$  is the Dirac  $\delta$ -function, defined as a generalised function.

Integrating (3.6)

$$\begin{aligned} \bar{u}v &= \frac{\pi}{2k} \frac{U''(y_c)}{U'(y_c)} v_0^2(y_c) & y < y_c \\ &= 0 & y > y_c \end{aligned} \quad (3.9)$$

where the boundary condition  $u \rightarrow U_\infty$ ,  $v \rightarrow 0$  as  $y \rightarrow \infty$  is used.

Also, direct from (3.1), (3.3)

$$\overline{uv} = -\frac{1}{2k} \frac{d\epsilon(y)}{dy} v_0^2(y)$$

Hence

$$\begin{aligned} \frac{d\epsilon(y)}{dy} v_0^2(y) &= -\pi \frac{u''(y_c)}{u'(y_c)} v_0^2(y_c) & y < y_c & \quad (3.10) \\ &= 0 & y > y_c & \end{aligned}$$

ie  $\frac{d\epsilon(y)}{dy} > 0$  for  $y < y_c$

and  $\epsilon(y) = \text{constant}$   $y > y_c$

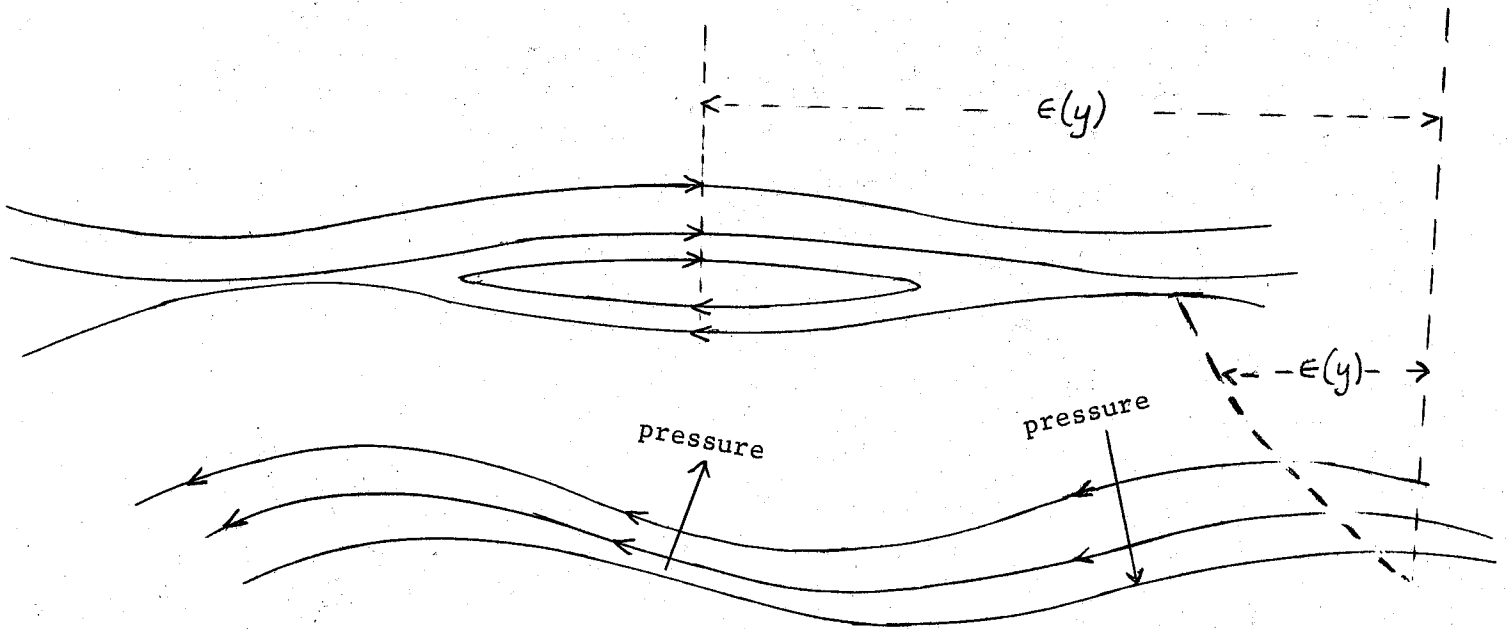
At  $y = y_c$ ,  $\epsilon(y)$  takes two values differing by  $\pi$ , depending on whether  $y_c$  is approached from above or below. This discontinuity is dictated by physical considerations, having the consequence that equation (3.1) must have the two solutions

$$v(y) = \pm v_0(y)$$

at the critical layer.

The streamline pattern, seen by an observer riding with the surface wave train, is shown in the figure.

The streamlines in the figure indicate the pressure distribution on the wave, and it is seen to be such as to cause a positive transfer of horizontal momentum from the air to the water waves. The critical layer has the 'catseye' structure, which also appears at the critical layer in stability problems, and it shows how this layer is one of concentrated vorticity.



We can now integrate equation (2.8) to give

$$\begin{aligned} \overline{u_1 v_1} + \overline{u_2 v_2} &= \nu \frac{dU}{dy} + \overline{u_2 v_2}_\infty & y > y_c \\ &= \nu \frac{dU}{dy} + \overline{u_2 v_2}_\infty + \frac{\pi}{R} \frac{U''(y_c)}{U'(y_c)} v_0^2(y_c) & y < y_c \end{aligned}$$

The total stress,  $\tau(x, y)$  is defined as

$$\tau(x, y) = \nu \frac{dU}{dy} - \overline{u v}^t$$

Hence

$$\begin{aligned} \overline{\tau}(x, y) &= -\overline{u_2 v_2}_\infty & y > y_c \\ &= -\overline{u_2 v_2}_\infty - \frac{\pi}{2R} \frac{U''(y_c)}{U'(y_c)} v_0^2(y_c) & y < y_c \end{aligned} \quad (3.11)$$

and all terms on the right of equations (3.11) are positive.

The stream function for the flow is

$$\psi = \frac{1}{k} v_0(y) \sin k(U-c)t \quad (3.12)$$

where

$$v = \frac{\partial \psi}{\partial x}, \quad u = -\frac{\partial \psi}{\partial y} + U(y)$$

Substitution in equation (2.9) gives

$$\frac{P}{\rho} = (U-c) \frac{\partial \psi}{\partial y} - U' \psi \quad (3.13)$$

and then replacing  $\psi$

$$\begin{aligned} \frac{P}{\rho} = & \left( \frac{U-c}{k} \frac{dv_0(y)}{dy} - \frac{1}{k} U'(y) v_0(y) \right) \sin k(U-c)t \\ & + \frac{U-c}{k} v_0(y) \frac{dU(y)}{dy} \cos k(U-c)t \end{aligned} \quad (3.14)$$

The part of the pressure containing  $\sin k(U-c)t$  is in phase with the displacement, and is the part which can lead to Kelvin-Helmholtz instability at the water surface. The term containing  $\cos k(U-c)t$  is in quadrature with the displacement, and describes the transfer of horizontal momentum from the air wave motion to the water wave motion. To obtain a measure of this transfer, consider the mean horizontal pressure component, which is

$$\overline{\frac{P}{\rho} \frac{\partial h}{\partial x}} = -\overline{uv} - \frac{\pi}{2k} v_0^2(y_c) \delta(y-y_c) \quad (3.15)$$

after some calculation. Thus, except at the critical layer, the horizontal component of the pressure is equal to the Reynolds stress.

The Rayleigh equation is

$$\frac{\partial^2 \psi}{\partial y^2} - k^2 \psi - \frac{U''}{U-c} \psi = 0 \quad (3.16)$$

Substituting for  $\psi$ , and reducing, obtain

$$\left( \frac{1}{k} \frac{d^2 v_0(y)}{dy^2} - \frac{1}{k} v_0(y) \left( \frac{dE(y)}{dy} \right)^2 - k v_0(y) - \frac{U''}{U-c} \frac{1}{k} v_0(y) \right) \sin k(U-c)t + \frac{\pi}{k} \frac{U''(y_c)}{U'(y_c)} v_0(y_c) \delta(y-y_c) = 0 \quad (3.17)$$

This curious equation becomes

for  $y > y_c$

$$\frac{d^2 v_0(y)}{dy^2} - k^2 v_0(y) - \frac{U''}{U-c} v_0(y) = 0 \quad (3.18)$$

for  $0 < y < y_c$

$$\frac{d^2 v_0(y)}{dy^2} - k^2 v_0(y) - \frac{U''}{U-c} v_0(y) - \frac{A^2}{(v_0(y))^3} = 0 \quad (3.19)$$

where  $A = \pi \frac{U''(y_c)}{U'(y_c)} v_0^2(y_c)$

The mean of the left hand side of (3.17) is zero for all  $y$ , including the critical layer, and the apparent time dependence disappears. The effect of the phase change appears explicitly in equation (3.19).

#### 4. Conclusions

The mean value in equations (3.7) is taken over  $t$  from  $t = 0$  to  $\infty$ , and presupposes that  $\frac{da}{dt} = 0$ . If instead, the mean value is taken from  $t = 0$  to  $T$ , as in equation (2.2), a broadened and slightly distorted  $\delta$ -function is obtained, leading to a distortion of the step function in equations (3.9), and a small difference in the algebraic results. However, the overall description of the flow remains unchanged, and it is a matter only of algebraic manipulation to make the correction.

The general effect of viscosity is to reduce velocity gradients. So it may be expected that the infinite gradients appearing at the critical layer would be reduced symmetrically, leaving a broadened  $\delta$ -function as a description of the loss of momentum from the mean air flow to the air wave flow. Dissipation would also lead to an increase in the area under this function, compared with the true  $\delta$ -function. The effect of viscosity on the normal stresses at the air-water interface is negligible, and viscosity becomes important only in the calculation of the tangential stresses.

To summarize: the concentrated vorticity at the critical layer causes transfer of horizontal momentum from the mean air motion to the air wave motion. This transfer may be described mathematically by the term  $\overline{p\omega v}$  in equation (3.6), which Lighthill (1962) called the vortex force, and showed its usefulness in

describing the physical processes at the critical layer.

This horizontal momentum is then carried down to the water waves as a Reynolds stress on the coupled wave motion in the air, and the air Reynolds stress is transmitted directly into the water Reynolds stress at the water surface. Equation (3.10) indicates that a necessary condition for the existence of such an air Reynolds stress is that the phase of the air wave motion is changing, ie  $\frac{d\epsilon(y)}{dy} \neq 0$ . The figure shows the stream lines produced by this type of motion, and makes it clear why an observer riding with the wave experiences a driving force from behind.

An equivalent description is to represent the air pressure at the water surface as being the real part of

$$P = (\alpha + i\beta) \rho U_1^2 k \eta \quad (4.1)$$

Equation (3.14) indicates how this representation is related to the flow characteristics.  $U_1$  here is a scaling velocity, and  $\alpha, \beta$  are functions of  $n$ , the wave frequency. This is the description taken by Miles (1957), and section 2 indicates that to obtain the total fluctuating pressure, one need only add to equation (4.1) the turbulent pressure fluctuations.

This investigation is a development of some of the ideas expressed by Dr. M. J. Lighthill in the lecture which is referred to below.

References

Lighthill (1962) Lecture delivered at the Applied Mechanics  
Conference, Bristol, April 1962.

Miles (1957) J. Fluid. Mech. 3, 185.

Phillips (1962) J. Geophys. Res., 67, 3135.

An Attempt to Simulate the Cromwell Current

in the Laboratory

by

James R. Holton

# An Attempt to simulate the Cromwell Current in the Laboratory.

James R. Holton

## 1. Introduction

The Cromwell Current, or equatorial undercurrent, is an intense ribbon-like zonal jet centered about the equator in the Pacific Ocean. The transport of the current is comparable to that of the Gulf Stream, yet its existence was not suspected until about ten years ago.

That the Cromwell Current has only recently been discovered is due, no doubt, to the paradoxical nature of the circulation in the equatorial Pacific. The surface water drifts slowly westward driven by the mean wind stress, but only a few meters below the surface the Cromwell Current flows eastward, with velocities of 50 to 150 cm/sec in its core at about 100 meters depth. The vertical scale of the current is about 200 meters, its latitudinal extent is about 1.5 degrees on either side of the equator, and its length is several thousand kilometers.

Because the core of this easterly current is at the equator its angular momentum exceeds that of the earth. This has led to occasional statements in the literature that a west to east pressure gradient is required to maintain the current against frictional dissipation. However, it would be possible to maintain an easterly current at the equator without a pressure gradient if there existed horizontal eddies which transferred net momentum equatorward through

a negative correlation of the velocities  $u'$ ,  $v'$  (where  $u'$  and  $v'$  are departures from the spatially averaged zonal and meridional velocities respectively). Similar eddies are important momentum transfer agents in the atmosphere and occur in quasi-geostrophic circulations when the streamlines are tilted so that  $u'$  is larger when  $v'$  is negative than when  $v'$  is positive. (See Figure 1).

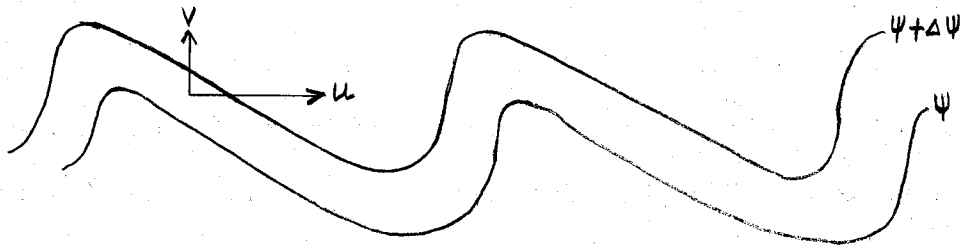


Figure 1.

Streamline field for net equatorward momentum flow.

To evaluate the possible importance of this momentum transport mechanism in the oceans would require synoptic observations which are not now available. Thus, in the studies of the Cromwell Current to date the zonal pressure gradient has been the explicit driving force and the eddy flux mechanism has not been considered. In fact, it is known from observations that a west to east pressure gradient does exist along the equator in the region of the Cromwell Current, and further, this pressure gradient disappears east of the Galapagos Islands, as does the Cromwell Current.

In view of the above discussion, it would be inappropriate to use an eddy viscosity coefficient to represent the effects of horizontal mixing, because not only the value, but even the sign of such a coefficient is in doubt for the larger eddy scales, and for the smaller scales the large vertical shear assures the dominance of vertical eddy dissipation.

## 2. A Physical Model of the Cromwell Current

The equation of motion for the steady state zonal component of the Cromwell Current may be written as,

$$u \frac{\partial u}{\partial x} + v \frac{\partial u}{\partial y} + w \frac{\partial u}{\partial z} - f v = - \frac{\partial p}{\partial x} + \nu \frac{\partial^2 u}{\partial z^2}$$

where  $\nu$  is the eddy coefficient of viscosity for vertical mixing and the other symbols have their usual meanings. At the equator  $f = 0$  and the above equation indicates that a balance will exist between the pressure force and the inertial and viscous terms. However, the extreme smallness of the Rossby number for large scale ocean circulations indicates that the circulation is quasigeostrophic even very close to the equator, and that the Cromwell Current may be an essentially geostrophic jet with an inerto-viscous boundary layer at the equator.

A possible model for the maintenance of this geostrophic current is the following. As shown by Stommel (Deep Sea Research 6) the mean easterly windstress creates a divergent surface Ekman layer at the equator, because the surface current is to the right of the

wind in the Northern Hemisphere and to the left in the Southern Hemisphere. This divergence forces an upwelling to preserve continuity. The upwelling and enhanced vertical mixing raise the thermocline at the equator and a core of cold dense water is maintained at 100 meters depth (see Figure 2).

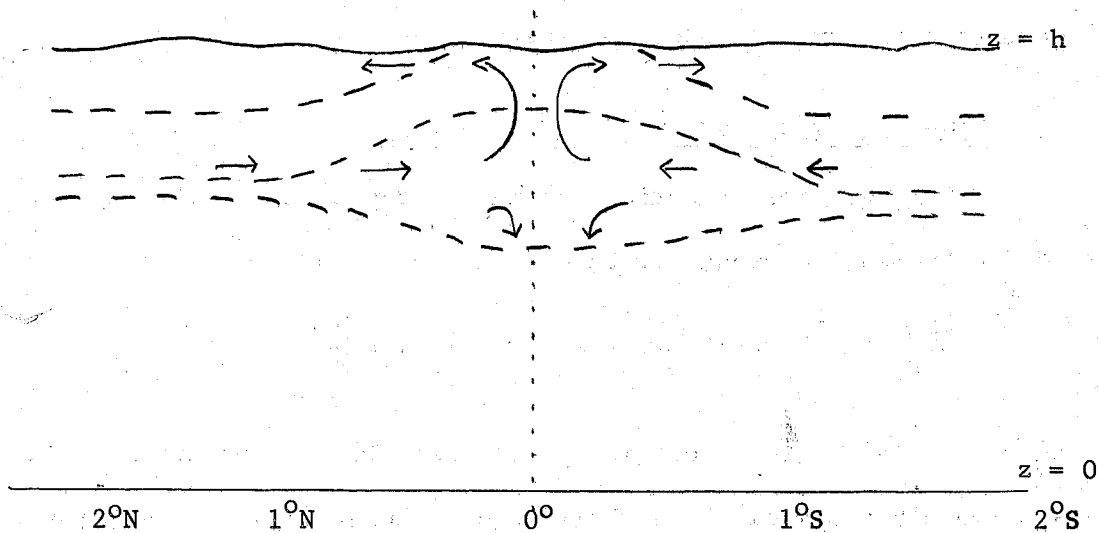


Figure 2.

Dashed lines represent isotherms. Arrows show the pattern of meridional circulation.

The result of this isotherm spread is a pressure gradient in the  $y$  direction pointed away from the equator in both hemispheres, which is balanced by an eastward moving geostrophic current.

In summary, it appears that three physical effects are necessary for the formation and maintenance of the equatorial undercurrent (1) the sign reversal of the Coriolis force, (2) a west to east pressure gradient, (3) divergence of the surface Ekman layer.

### 3. A Possible Laboratory Analogy to the Cromwell Current

In the rotating dishpan it is not possible to model the sign change of the Coriolis force. However, the author thought that it might be possible to produce a current analogous to the Cromwell Current along the outer radial boundary wall of a sixty degree cylindrical sector which had previously been used by Dr. Fallor for modelling ocean circulations. This sector was placed in the large rotating tank with its apex at the center of the tank. A wind stress was applied in the clockwise direction as the tank was rotated counterclockwise. A two-layer fluid system was used in the sector, with the less dense fluid at the top. The qualitative expectation was that the surface Ekman divergence at the equatorial rim (forced by the kinematic constraint of the wall) would create a vertical upwelling to preserve continuity. In a matter analogous to the Cromwell Current this effect was expected to raise the level of the denser layer near the rim and create a radially inward pressure gradient which together with the zonal pressure gradient caused by water piling up at the western boundary would force an easterly quasigeostrophic current along the wall. Note that since the Coriolis force doesn't change signs the presence of the wall is necessary to the formation of a jet, otherwise the Ekman layer divergence would tend to produce a vortex. The proposed model is indicated schematically in Figure 3.

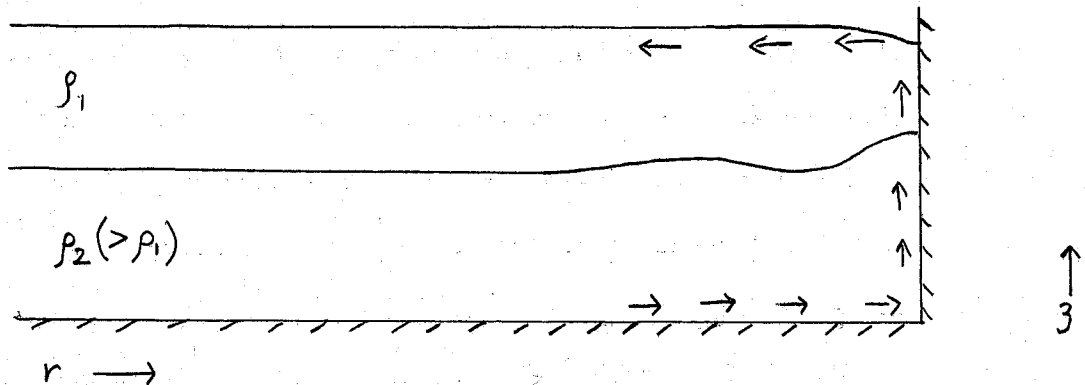


Figure 3.

Arrows indicate the meridional circulation.

#### 4. The Experimental Procedure

The wind stress was first calibrated by using the full cylindrical tank to obtain velocity profiles as a function of radius. From the theory of Ekman boundary layers it may be shown that

$$\tau_{\theta} = f \nu^{1/2} \Omega^{1/2} V_{\theta}$$

where  $\tau_{\theta}$ ,  $V_{\theta}$  are the wind stress and velocity is the zonal direction. Eight stationary blowers were used to adjust the wind stress so that  $\frac{\partial \tau_{\theta}}{\partial y}$  fit a sine curve to a reasonable approximation.

As a control experiment the sector was used with a wind stress driving force and a single homogeneous layer of water. A western boundary current was produced as predicted by Stommel's theory of western intensification. The flow pattern is indicated schematically in Figure 4.

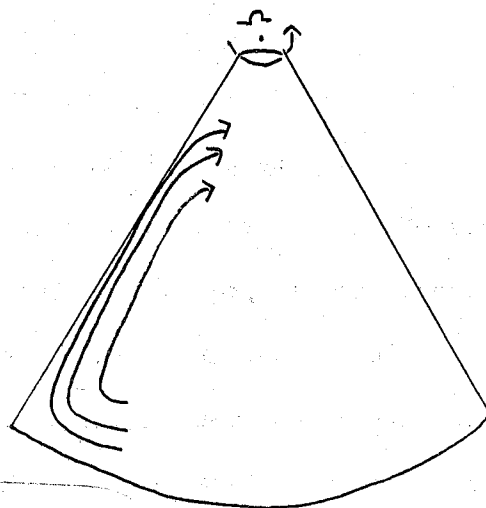


Figure 4.

It is an interesting digression to compare quantitatively the western boundary current experimentally observed with the prediction of Stommel's theory (see Trans. of A.G.U. 29). For the experimental system the conservation of potential vorticity may be written

$$R \nabla^2 \psi + \beta \frac{\partial \psi}{\partial x} = -\frac{1}{f} \frac{\partial \zeta_x}{\partial y}$$

where  $\psi$  is a geostrophic stream function  $R = \sqrt{\frac{\nu}{2f}}$ , and  $\beta = \frac{\Omega^2 r_0}{2g}$  approximates the mean change of the free surface height in the radial direction due to rotation. This equation simply states that the vorticity gain due to wind stress curl equals the vorticity loss due to frictional drag at the bottom plus the vorticity change due to the change of height in fluid columns moving in the meridional direction. This equation is

easily solved only for a rectangular basin, but it has been shown by Munk and Carrier (Tellus 2) that a triangular geometry produces only small quantitative differences in the circulation.

The width of the observed western boundary current agreed well with the theoretically predicted value of 3 cm. (The sector radius was 100 cm. and the rotation rate was 8.23 r.p.m. for these experiments)) However, the observed velocity in the boundary current of 1 cm/sec was only half the value predicted by the theory. For better quantitative predictions it is apparently not permissible to neglect the dissipation against the side boundary and the inertial terms as done in the above theory.

Experiments were then conducted with a two layer system. This system was produced by filling the sector with 6 cm. of fresh water, then slowly adding a one percent solution of barium chloride through a glass tube whose outlet was one mm. above the bottom boundary. With a flow rate of about 100 cc/min a sharp interface could be achieved with the salt solution spreading out along the bottom.

In all wind stress experiments with the sector the main tank was filled up to the rim of the sector (13 cm depth) to eliminate the possibility of eddies caused by the flow of air over the sector walls.

The rotation rate and stratification were selected to attempt to meet the similarity requirements of equality of the

Rossby number and Richardson number in the model and the prototype.

For the ocean the Richardson number is approximately:

$$Ri_p = \frac{g \alpha T L_z}{u^2} = \frac{(10^3)(2 \times 10^{-4})(20)(2 \times 10^4)}{(50)^2} = 40$$

Whereas in the model if a salt concentration of 10 gm/litre and a rotation rate of 5 r.p.m. are used the Richardson number is given by

$$Ri_m = \frac{g S L_z}{u^2} = \frac{(10^3)(.01)(5)}{(1)^2} = 50$$

where  $S$  denotes gms. salt per gm. of water.

The Rossby number ( $\equiv u/2\Omega L$ ) is estimated to be of the order  $10^{-2}$  in the equatorial oceans (except extremely close to the equator where  $\Omega \rightarrow 0$ ). If  $u = 1$  cm/sec is a typical velocity scale in the model similarity would require a rotation rate of 5 r.p.m.

#### 5. Results of the Two Layer Experiments.

Various conditions of wind stress and rotation rate were used in an attempt to observe a boundary current along the equatorial rim. In most cases the results were negative. A few instances of transient counter currents were observed, but these were no doubt a result of thermal circulations due to heating or cooling at the walls. Numerous difficulties were encountered in working with the two layer model. It required several hours to produce the desired two layer system, then the system had to be accelerated up

to 5 r.p.m. at an extremely slow rate to prevent turbulent mixing of the layers. Another few hours were required for the primordial baroclinic circulations to disappear. In fact, in most cases the experiment had to be abandoned before a steady state was reached.

In only one experiment was a steady state definitely achieved. In that case the rotation rate was 5 r.p.m. and no blowers were used, so that the only wind stress was that due to the relative motion of the tank. The steady state circulation showed no evidence of an equatorial boundary current. In the top layer there was a nearly symmetric gyre driven by the wind with a mean velocity of 1 cm/sec. In the bottom layer the motion was very slow (nearly an order of magnitude less than the top layer) indicating nearly complete pressure compensation due to a sloping interface.

One possible explanation of the failure of these experiments is that the wind stress applied to the surface may serve to continually excite baroclinic instability so that transient motions will always dominate the system. Longer experiments at very uniform temperature and humidity conditions would be needed to test this hypothesis. However, the evidence to date seems to vitiate the hope of finding a boundary current analogous to the Cromwell Current in the system described.

#### References

Several papers dealing with the Cromwell Current may be found in Deep Sea Research 6 (1960).

Baroclinic Instability in Two Layer Systems

by

Joseph Pedlosky

# Baroclinic Instability in Two Layer Systems

Joseph Pedlosky

## Introduction

In the dynamics of atmospheric and oceanic systems an important role is played by the release of energy by dynamically unstable mean flow systems. What is usually meant by such mean systems is a flow with negligible zonal variation. The perturbations which grow from such unstable systems have fundamentally two energy sources, the horizontal (north-south) shear of the mean motion, and the available potential energy associated with a north-south density gradient and a vertical shear.

One of the simplest physically reproducible models that contains these elements is the two layer system shown here in Fig. 1.

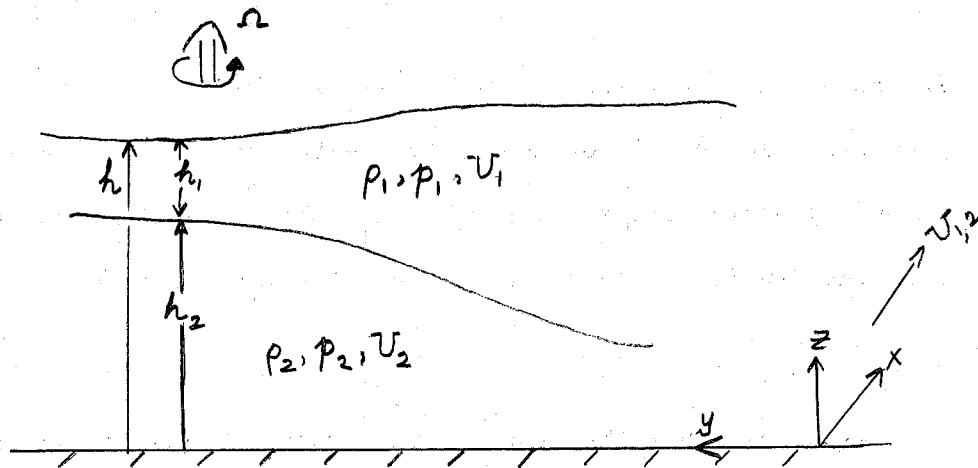


Fig. 1

The flow is taken to be gravitationally stable ( $\rho_1 < \rho_2$ ) and the pressure is determined hydrostatically while  $\rho$  is constant in each layer.

$$(1) \quad (a) \quad p_1 = \rho_1 g(h - z) \quad h > z > h_2$$

$$(b) \quad p_2 = \rho_2(h_2 - z)g + \rho_1 g h_1 \quad h_2 > z > 0$$

Consider a situation where the flow in the system is only in the x direction and is a function of y only and is geostrophically balanced

$$(2) \quad (a) \quad \rho_1 f u_1 = - \frac{\partial p_1}{\partial y} = - \rho_1 g \frac{\partial h}{\partial y}$$

$$(b) \quad u_1 = - \frac{g}{f} \frac{\partial h}{\partial y}$$

If  $u_2 = 0$

$$(3) \quad (a) \quad \frac{\partial p_2}{\partial y} = 0 = \rho_1 g \frac{\partial h_1}{\partial y} + \rho_2 g \frac{\partial h_2}{\partial y} = \rho_1 g \frac{\partial h}{\partial y} + \frac{\rho_2 - \rho_1}{\rho_2} \rho_2 g \frac{\partial h_2}{\partial y}$$

$$(b) \quad \frac{\partial h_2}{\partial y} = - \frac{\rho_1}{\rho_2 - \rho_1} \frac{\partial h}{\partial y} = + \frac{\rho_1}{\Delta \rho} \frac{f}{g} u_1$$

In the usual case where  $\frac{\Delta \rho}{\rho} \ll 1$  we see that a vertical shear produces a large tilt of the interface between the two layers and an energy source for the disturbance. The lines of constant pressure and density are not parallel and the flow is baroclinic.

### I Equations of Motion

One can show that for a layer system the equations of motion in each layer are the conservation of potential vorticity and the conservation of volume.

$$(1.1) \quad (a) \quad \frac{D}{Dt} \left( \frac{\xi + f}{h} \right) = 0$$

$$(b) \quad \frac{D}{Dt} (h) + h \operatorname{div} \vec{u} = 0$$

where  $h$  is the layer thickness,  $\xi = v_x - u_y$ , and  $D/Dt$  is the two dimensional substantial derivative.

The system becomes closed if we assume that the frequency scale of the motion  $\frac{U}{L}$  ( $U$  is a characteristic velocity and  $L$  a characteristic length) is small compared to the earth rotation frequency  $f/2$ . In such systems the flow is geostrophically balanced during the motion and

$$(1.2) \quad \xi = v_x - u_y = \frac{p_{xx}}{\rho f} + \frac{p_{yy}}{\rho f}$$

this assumption with the assumption of hydrostatic vertical balance closes the system.

For the mean state whose stability we wish to investigate we take:  $\bar{u}_1 = \bar{u}_1(y)$ ,  $\bar{u}_2 = \bar{u}_2(y)$ ;  $\bar{v}_2 = \bar{v}_1 = 0$ . We superimpose small perturbations on the system of the form: ( $h$  is to total height)

$$(1.3) \quad \begin{aligned} h &= h(y) e^{ik(x-ct)} \\ h_1 &= h_1(y) e^{ik(x-ct)} \quad \text{etc.} \end{aligned}$$

In these expressions  $c$  is in general a complex number and the linearized perturbation equations corresponding to (1.1) are

$$(1.4) \quad \begin{aligned} (a) \quad (\bar{u}_1 - c)(D^2 - k^2)p_1 + (\beta - \bar{u}_{1yy} - \frac{H_{1y}}{H_1})p_1 &= \frac{f^2}{g'H_1}(\bar{u}_1 - c)(p_1 - p_2) \\ (b) \quad (\bar{u}_2 - c)(D^2 - k^2)p_2 + (\beta - \bar{u}_{2yy} - \frac{H_{2y}}{H_2})p_2 &= \frac{f^2}{g'H_2}(\bar{u}_2 - c)(p_2 - p_1) \end{aligned}$$

where  $h_1 = \frac{p_1 - p_2}{\rho_2 g'}$

$$h = \frac{p_1}{\rho g}, \quad D \equiv \frac{d}{dy}, \quad g' = \Delta P / \rho g$$

and we have assumed  $\frac{\Delta p}{p} \ll 1$ .

If we scale the variables in the following manner:

$$(x, y) = (x', y') L \quad k = \alpha / L$$

$$\bar{u}_{(1,2)} = U_0 \bar{u}'_{(1,2)} \quad c = U_0 c'$$

$$H_y = \frac{U_0 f}{g'} H'_2 y$$

The non-dimensional equations are (after dropping the primes)

$$(1.5) \quad (a) \quad (D^2 - \alpha^2) p_1 + (\beta / R_0 - u_{1yy} - F_1 H_{1y}) \frac{p_1}{(U_1 - c)} - F_1 p_1 = -F_1 p_2$$

$$(b) \quad (D^2 - \alpha^2) p_2 + (\beta / R_0 - u_{2yy} - F_2 H_{2y}) \frac{p_2}{(U_2 - c)} - F_2 p_2 = -F_2 p_1$$

$$F_{1,2} = \frac{f^2 L^2}{g' H_{1,2}} = \frac{f^2 L^2}{U_0^2} \frac{U_0^2}{g' H_{1,2}} = \left(\frac{1}{R_0}\right)^2 F_{R_{1,2}}^*$$

$$R_0 = \frac{U_0}{f L}$$

$$F_{R_{1,2}} = \frac{U_0^2}{g' H_{1,2}}$$

For convenience define the y derivative of the mean potential vorticity in the  $c^{\text{th}}$  layer as:

$$\frac{\partial q_i}{\partial y} \equiv \left( \beta / R_0 - u_{iyy} - F_i H_{iy} \right)$$

\*

If  $F_{1,2}$  is of order unity we see that the mean flow is subcritical in the hydraulic sense.

The phase velocity  $c$  is in general complex,  $c = c_r + i c_i$   
 ( $c_r$  and  $c_i$  real) and the flow is unstable if  $c_i > 0$ .

## II. Necessary Conditions for Instability

The perturbation equations can be written as

$$(2.1) \quad (a) \quad (D^2 - \alpha^2) p_1 + \frac{\partial q_1}{\partial y} \frac{p_1}{U_1 - c} - F_1 p_1 = -F_1 p_2$$

$$(b) \quad (D^2 - \alpha^2) p_2 + \frac{\partial q_2}{\partial y} \frac{p_2}{U_2 - c} - F_2 p_2 = -F_2 p_1$$

Multiply (2.1)(a) by  $p_1^*$  (complex conjugate of  $p_1$ ) and subtract from that the conjugated equation to obtain

$$(2.2) \quad (a) \quad \frac{d}{dy} \left( p_1^* \frac{dp_1}{dy} - p_1 \frac{dp_1^*}{dy} \right) + 2 c_i \frac{\partial q_1}{\partial y} \frac{|p_1|^2}{|U_1 - c|^2} = -F_1 (p_2 p_1^* - p_1 p_2^*)$$

Similarly for layer two

$$(b) \quad \frac{d}{dy} \left( p_2^* \frac{dp_2}{dy} - p_2 \frac{dp_2^*}{dy} \right) + 2 c_i \frac{\partial q_2}{\partial y} \frac{|p_2|^2}{|U_2 - c|^2} = -F_2 (p_1 p_2^* - p_2 p_1^*)$$

Integrate (2.2)(a) and (b) between two points  $y_1$  and  $y_2$  where  $p_1$  and  $p_2$  go to zero. We eliminate the coupling term on the right hand side and obtain (where  $c = c_r + i c_i$ )

$$2 c_i \left[ \int_{y_1}^{y_2} \frac{\partial q_1}{\partial y} \frac{|p_1|^2}{|U_1 - c|^2} + \frac{\partial q_2}{\partial y} \frac{|p_2|^2}{|U_2 - c|^2} \right] = 0$$

or

$$(2.3) \quad \boxed{2 c_i \int_{y_1}^{y_2} \sum_{m=1}^2 H_m \frac{\partial q_m}{\partial y} \frac{|p_m|^2}{|U_m - c|^2} = 0}$$

Therefore if  $c_i \neq 0$  the potential vorticity must be positive in some regions and negative in others for instability to occur. It is not true that it must be zero some place in the fluid since the flow is discontinuous. It is clear also that equation (2.3) can be generalized to any multiple layer model. In the simplest baroclinic model where horizontal shears are neglected as well as  $\beta$

$$\frac{\partial q_1}{\partial y} = -F_1 H_1 y > 0 \text{ and constant}$$

$$\frac{\partial q_2}{\partial y} = -F_2 H_2 y < 0 \text{ and constant}$$

In the case where  $\Delta\rho/\rho \ll 1$   $H_{1y} \approx -H_2 y$  equation (2.3) tells us then that

$$(2.4) \quad -\frac{|p_1|^2}{|U_1 - c|^2} + \frac{|p_2|^2}{|U_2 - c|^2} = 0$$

or

$$\frac{|p_1|^2}{|p_2|^2} = \frac{|U_1 - c|^2}{|U_2 - c|^2} = \frac{|U_{1 \text{ rel}}|^2}{|U_{2 \text{ rel}}|^2} = K_1$$

so that

$$(2.5) \quad |p_i|^2 = K |U_{\text{rel}}|^2$$

and the amplitude of the pressure perturbation in each layer is proportional to the relative wind in that layer.

Consider the case where neglecting  $\beta$ ,  $\frac{\partial q_1}{\partial y} = 0$  and  $u_2 = 0$ :

$$+ \frac{d^2 u_1}{dy^2} - F_1 u_1 = 0$$

since in non-dimensional units  $H_1 y = -u_1$ .

So that in a region with a wall (at  $y = 0$ ) marking the northernmost extent of the fluid:

$$u_1 \approx e^{+\sqrt{F_1} y} \quad -\infty \leq y \leq 0$$

Now

$H_2 y = -H_1 y = u_1$ , and does not change sign so that equation (2.3) yields  $c_i = 0$ , and the flow is stable. However let us consider putting into our system a bottom slope of the form

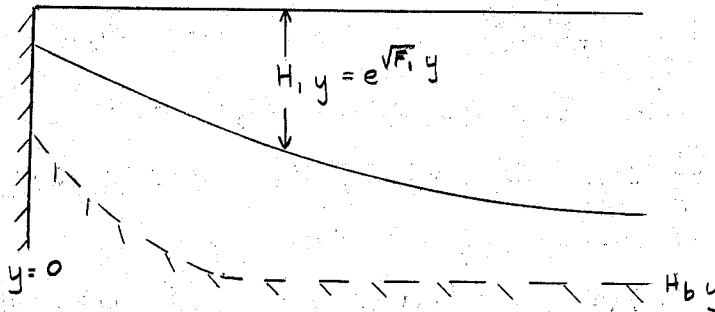


Fig. 2

shown in Figure 2.

In this case if the bottom slope is chosen correctly, the flow will satisfy the necessary condition for instability. So the addition of a bottom slope which is in this case in the  $\beta$  "sense" appears to be a destabilizing influence. In any case, we

can arbitrarily change the potential vorticity in the lowest layer, thus changing the stability properties of the flow, without altering the kinematics of the mean flow, (e.g.) a symmetric flow over a symmetric (in  $y$ ) mountain will have asymmetric stability properties, the flow being more unstable on the northern slope for a westerly shear.

Let us define the following functions for the unstable flow regime

$$(2.6) \quad \phi_1 = \frac{p_1}{u_1 - c} \quad ; \quad \phi_2 = \frac{p_2}{u_2 - c}$$

Then equations (2.1) may be re-written as (if we ignore  $\beta$ )

$$(2.7) \text{ (a)} \quad \frac{\partial}{\partial y} \frac{(u_1 - c)^2}{F_1} \frac{d\phi_1}{dy} - \alpha^2 \frac{(u_1 - c)^2}{F_1} \phi_1 + (u_1 - c)(u_1 - u_2) \phi_1 = (u_1 - c)(p_1 - p_2) = \\ = (u_2 - c)(u_1 - c)(\phi_1 - \phi_2) + (u_1 - u_2) \phi_1 (u_1 - c)$$

$$(2.7) \text{ (b)} \quad \frac{\partial}{\partial y} \frac{(u_2 - c)^2}{F_2} \frac{d\phi_2}{dy} - \alpha^2 \frac{(u_2 - c)^2}{F_2} \phi_2 + (u_2 - c)(u_2 - u_1) \phi_2 = (u_2 - c)(p_2 - p_1) = \\ = (u_1 - c)(u_2 - c)(\phi_2 - \phi_1) + (u_2 - u_1) \phi_2 (u_2 - c)$$

multiply (2.7) (a) by  $\phi_1^*$  and (2.7) (b) by  $\phi_2^*$  and integrate between  $y_1$  and  $y_2$ , and add the resulting equations

$$(2.8) \quad - \int_{y_1}^{y_2} dy \left\{ \frac{(u_1 - c)^2}{F_1} \left[ \left| \frac{d\phi_1}{dy} \right|^2 + \alpha^2 |\phi_1|^2 \right] + \frac{(u_2 - c)^2}{F_2} \left[ \left| \frac{d\phi_2}{dy} \right|^2 + \alpha^2 |\phi_2|^2 \right] \right\} = \\ = \int_{y_1}^{y_2} (u_1 - c)(u_2 - c) \left\{ |\phi_1|^2 - \phi_2 \phi_1^* - \phi_1 \phi_2^* + |\phi_2|^2 \right\} dy \\ = \int_{y_1}^{y_2} (u_1 - c)(u_2 - c) |\phi_1 - \phi_2|^2 dy \\ = - \int_{y_1}^{y_2} \left\{ [(u_1 - c) - (u_2 - c)]^2 - (u_1 - c)^2 - (u_2 - c)^2 \right\} \frac{|\phi_1 - \phi_2|^2}{2} dy$$

$$(2.9) \quad + \int_{y_1}^{y_2} dy (u_1 - c)^2 [\varphi_1] + \int_{y_1}^{y_2} dy (u_2 - c)^2 [\varphi_2] = + \int_{y_1}^{y_2} (u_1 - u_2)^2 J dy$$

where  $\varphi_1$ ,  $\varphi_2$  and  $J$  are positive definite quantities.

The imaginary part of (2.9) is

$$(2.10) \quad c_i \int_{y_1}^{y_2} (u_1 - c_i) \varphi_1 dy + \int_{y_1}^{y_2} (u_2 - c_i) \varphi_2 dy = 0$$

The real part of (2.9) yields:

$$(2.11) \quad \int_{y_1}^{y_2} u_1^2 \varphi_1 dy + \int_{y_1}^{y_2} u_2^2 \varphi_2 dy - 2c_i \int_{y_1}^{y_2} (\varphi_1 u_1 + \varphi_2 u_2) dy + c_i^2 \int_{y_1}^{y_2} (\varphi_1 + \varphi_2) dy \\ - c_i^2 \int_{y_1}^{y_2} (\varphi_1 + \varphi_2) dy = \int_{y_1}^{y_2} (u_2 - u_1)^2 J dy$$

Let a bar denote integration between  $y_1$  and  $y_2$ .

Then using (2.10), (2.11) becomes

$$(2.12) \quad \overline{u_1^2 \varphi_1} + \overline{u_2^2 \varphi_2} = (c_i^2 + c_i^2) (\overline{\varphi_1 + \varphi_2}) + \overline{(u_2 - u_1)^2 J}$$

Now let both  $u_1$  and  $u_2$  be bounded from above by  $a$  and from below by  $b$ . Then the following inequality holds

$$(2.13) \quad 0 \geq \overline{(u_1 - a)(u_1 - b) \varphi_1} + \overline{(u_2 - a)(u_2 - b) \varphi_2} = \\ = \overline{u_1^2 \varphi_1} + \overline{u_2^2 \varphi_2} - (\overline{u_1 \varphi_1} + \overline{u_2 \varphi_2})(a + b) + ab \overline{(\varphi_1 + \varphi_2)}$$

Substituting from (2.10) and (2.13):

$$(2.14) \quad 0 \geq (c_n^2 + c_i^2) \overline{(q_1 + q_2)} - c_n(a+b) \overline{(q_1 + q_2)} + ab \overline{(q_1 + q_2)} + \overline{(u_2 - u_1)^2} \overline{J}$$

or equivalently, since  $\overline{(u_2 - u_1)^2} \overline{J} \geq 0$

$$(2.15) \quad \left(\frac{a-b}{2}\right)^2 \geq \left(c_n - \left(\frac{a+b}{2}\right)\right)^2 + c_i^2$$

The complex phase speed lies within a semicircle of diameter  $a - b$  (the difference between the velocity extremes) and the circle is centered on the real axis at  $\frac{a+b}{2}$  the median velocity (Fig. 3).

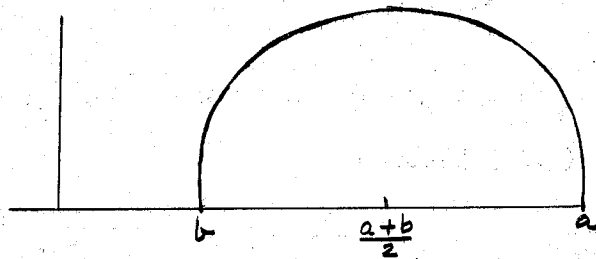


Fig. 3. (semicircle which contains phase speed)

This type theorem was first proven by Howard for continuously stratified shear flows in two dimensional flow in which the horizontal divergence is zero.

We can do a little more with this. Let

$$(2.16) \quad (a) \quad \begin{aligned} b_1 &\leq u_1 \leq a_1 \\ b_2 &\leq u_2 \leq a_2 \end{aligned}$$

Then instead of (2.13) we have:

$$(2.16) (b) \quad 0 \geq \overline{u_1^2 \varrho_1} + \overline{u_2^2 \varrho_2} - \overline{u_1 \varrho_1 (a_1 + b_1)} - \overline{u_2 \varrho_2 (a_2 + b_2)} + \overline{a_1 b_1 \varrho_1} + \overline{a_2 b_2 \varrho_2}$$

or using the relations (2.10) and (2.11)

$$(2.16) (c) \quad 0 \geq (\overline{C_1^2} + \overline{C_2^2})(\overline{\varrho_1 + \varrho_2}) - \overline{(a_1 + b_1) C_1 (\varrho_1 + \varrho_2)} + \overline{a_1 b_1 (\varrho_1 + \varrho_2)} \\ + \overline{u_2 \varrho_2 (a_1 + b_1 - (a_2 + b_2 - (a_2 + b_2)))} \\ + \overline{\varrho_2 (a_2 b_2 - a_1 b_1)}$$

The inequality in (2.14) is still valid if  $u_2$  is replaced by its minimum value  $b_2$ , if  $a_1 + b_1 \geq a_2 + b_2$  and if  $a_1 + b_1 > 0$  (i.e. if the median value in layer 1 is greater than that in layer 2).

$$(2.17) \quad \left( C_1 - \frac{a_1 + b_1}{2} \right)^2 + C_2^2 \leq \left( \frac{a_1 - b_1}{2} \right)^2 + \frac{\overline{\varrho_2}}{\overline{\varrho_1 + \varrho_2}} (a_1 - b_2)(b_1 - b_2)$$

If  $b_1 = b_2$  (2.17) reduces to (2.15) since  $a_1$  and  $b_1$  are then the velocity bounds for both layers.

Consider the following case:

$$b_1 < b_2$$

$$a_1 >> a_2$$

Equation (2.15) would yield a semicircle bound as indicated by the figure below.

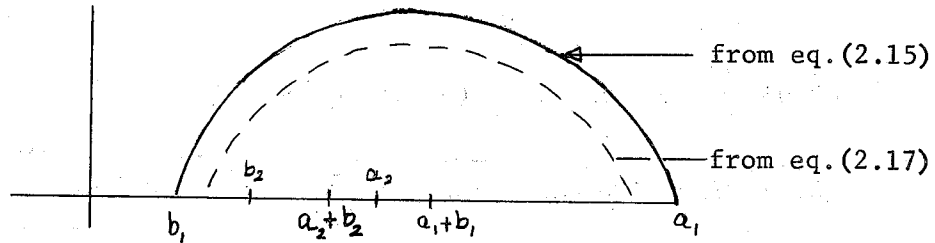


Fig. 4

Equation (2.17) tells us that the limiting bound is actually less since  $\frac{\overline{\vartheta_2}}{\overline{\vartheta_1 + \vartheta_2}} (a_1 - b_2)(b_1 - b_2) \leq 0$ . If  $b_2 < b_1$  then we have a limiting semicircle whose diameter is larger than in the case  $b_2 > b_1$ . This implies the flow is more unstable (or is at least capable of greater growth rates) if the minimum value of the velocity is in the lower layer and the maximum in the upper layer, a not very surprising result.

If  $\beta$  is reintroduced in the potential vorticity, equation (2.10) becomes ( $C_i \neq 0$ ),

$$(2.18) \quad C_n (\overline{\vartheta_1 + \vartheta_2}) = \overline{u_1 \vartheta_1} + \overline{u_2 \vartheta_2} - \beta \left\{ \frac{|\phi_1|^2 + |\phi_2|^2}{2} \right\}$$

equation (2.12) (a) becomes:

$$(2.19) \quad \overline{u_1^2 \vartheta_1} + \overline{u_2^2 \vartheta_2} = \overline{(u_1 - u_2)^2 J} + (C_n^2 + C_i^2) (\overline{\vartheta_1 + \vartheta_2}) + \beta (\overline{u_1 |\phi_1|^2} + \overline{u_2 |\phi_2|^2})$$

Finally equation (2.15) becomes

$$(2.20) \quad \left( \frac{a-b}{2} \right)^2 \geq \left\{ C_n - \frac{a+b}{2} \right\}^2 + C_i^2 + \frac{\beta}{\overline{\vartheta_1 + \vartheta_2}} \left[ \overline{\left( u_1 + \frac{a+b}{2} \right) |\phi_1|^2} + \overline{\left( u_2 + \frac{a+b}{2} \right) |\phi_2|^2} \right]$$

If  $u_1 \geq 0$  and  $u_2 \geq 0$  the semicircle theorem (equation (2.15)) is still valid for the problem when  $\beta \neq 0$ . The semicircle diameter will be smaller (but never larger) than the bound given by (2.15) especially for  $\alpha$  small.

### III Sufficient Conditions for Instability

Consider the class of flows for which there exists extrema of the vorticity in layer 1 and the velocity is zero in layer 2. Further let the extrema in layer 1 occur for a point or points of constant velocity ( $u_1 = C_S$ ). If:

$$(3.1) \quad 0 \leq \frac{\partial q_1 / \partial y}{u_1 - C_S} \equiv K_1(y) < \infty$$

$$(3.2) \quad 0 < \frac{\partial q_2 / \partial y}{-C_S} \equiv K_2(y) < \infty$$

then we can show that a neutral solution of equations (2.1) exists with phase speed  $C_S$ .

Consider the functional  $A^2$  defined by

$$(3.3) \quad A^2 = \frac{\int_{y_1}^{y_2} dy \left[ \frac{K_1(y)}{F_1} (p_1)^2 - (p_1 - p_2) \left( \frac{\partial p_1}{\partial y} \right)^2 \frac{1}{F_1} - \left( \frac{\partial p_2}{\partial y} \right)^2 \frac{1}{F_2} + \frac{K_2(y)}{F_2} (p_2)^2 \right]}{\int_{y_1}^{y_2} dy \left( \frac{p_1^2}{F_1} + \frac{p_2^2}{F_2} \right)}$$

$A^2$  possesses a maximum  $\leq K_{1 \max} + K_{2 \max}$  which is positive.

This maximum occurs where  $\frac{\delta A^2}{\delta p_1} = 0$  and  $\frac{\delta A^2}{\delta p_2} = 0$ . These variational conditions are equivalent to the equations (2.1)(a) and (b)

if  $A_{\max}^2$  is associated with  $\alpha^2$  and  $C = C_S$ . A neutral solution

therefore exists for  $\hat{\alpha} = A_{\max}$  and  $C = C_S$  and  $p = \hat{p}$  satisfying the

equations

$$(3.4) \text{ (a)} \quad (D^2 - \hat{\alpha}^2) \hat{p}_1 + \frac{\partial q_1}{\partial y} \frac{\hat{p}_1}{U_1 - c} - F_1 \hat{p}_1 = -F_1 \hat{p}_2$$

$$(3.4) \text{ (b)} \quad (D^2 - \hat{\alpha}^2) \hat{p}_2 + \frac{\partial q_2}{\partial y} \frac{\hat{p}_2}{U_2 - c} - F_1 \hat{p}_2 = -F_2 \hat{p}_2$$

Consider some disturbance at a wave number  $\alpha$  near  $\hat{\alpha}$ .

$$(3.5) \text{ (a)} \quad (D^2 - \alpha^2) p_1 + \frac{\partial q_1}{\partial y} \frac{p_1}{U_1 - c} - F_1 p_1 = -F_1 p_2$$

$$(3.5) \text{ (b)} \quad (D^2 - \alpha^2) p_2 + \frac{\partial q_2}{\partial y} \frac{p_2}{U_2 - c} - F_2 p_2 = -F_2 p_1$$

Multiply (3.4) (a) by  $\hat{p}_1$ , (3.4) (b) by  $\hat{p}_2$ ; (3.5) (a) by  $p_1$  and (3.5) (b) by  $p_2$  and obtain after integration over the range

$(y_1, y_2)$ :

$$(3.6) \quad 0 = \frac{1}{F_1} (\alpha^2 - \hat{\alpha}^2) \overline{p_1 \hat{p}_1} + \frac{1}{F_2} (\alpha^2 - \hat{\alpha}^2) \overline{p_2 \hat{p}_2} + \frac{\partial q_1}{\partial y} \overline{p_1 \hat{p}_1} \frac{C_s - c}{(U_1 - c)(U_1 - C_s)} + \frac{\partial q_2}{\partial y} \frac{\overline{p_2 \hat{p}_2} (C - C_s)}{(U_2 - c)(U_2 - C_s)}$$

or

$$(3.7) \quad \frac{\alpha^2 - \hat{\alpha}^2}{C - C_s} = \frac{\overline{K_1(y) p_1 \hat{p}_1}}{F_1 (U_1 - c)} + \frac{\overline{K_2(y) p_2 \hat{p}_2}}{F_2 (U_2 - c)}$$

$$\frac{\overline{p_1 \hat{p}_1}}{F_1} + \frac{\overline{p_2 \hat{p}_2}}{F_2}$$

Now let  $\alpha^2 \rightarrow \hat{\alpha}^2$ ;  $C \rightarrow C_s$  such that  $\text{Im } c > 0$ .

One obtains

$$(3.8) \quad \left( \frac{d\alpha^2}{dc} \right)_{c=c_0} = \lim_{c_i \rightarrow 0} \frac{\frac{K_1(y) (\hat{p}_1)^2}{F_1 (U_1 - c)} + \frac{K_2(y) (\hat{p}_2)^2}{F_2 (U_2 - c)}}{\frac{(\hat{p}_1)^2}{F_1} + \frac{(\hat{p}_2)^2}{F_2}}$$

These integrals are discussed by Lin (1955) where it is shown then that

$$(3.9) \quad \left( \frac{d\alpha^2}{dc} \right)_{c=c_0} = A + iB$$

where all that is important is that  $B > 0$ ,  $A$  and  $B$  bounded.

We see that

$$(3.10) \quad \frac{dc}{d\alpha^2} = \frac{A - iB}{A^2 + B^2}$$

So that if  $\alpha^2$  decreases slightly  $C_0$  becomes positive and the flow is unstable to wavelengths slightly longer than  $\hat{L}^2 = \left( \frac{2\pi}{\alpha} \right)^2$ .

As an example consider the flow (in non-dimensional units)

$$(3.11) \quad u_1 = e^{-r^2 y^2}$$

Now

$$(3.12) (a) \quad \frac{\partial q_1}{\partial y} = (2r^2 + F_1 - r^4 y^2) e^{-y^2}$$

$$(b) \quad \frac{\partial q_2}{\partial y} = -F_2 e^{-r^2 y^2}$$

The potential vorticity in the top layer vanishes at

$$y_c = \pm \frac{\sqrt{F_1 + 2r^2}}{2r^2}. \quad \text{We see that this jet flow satisfies the criteria}$$

listed at the beginning of this section so that a neutral solution

exists with a phase speed  $C_s = e^{(F_1 + 2r^2)}$  and a neighboring unstable solution also exists.

We have tacitly assumed that  $y_c$  lies in the interval of the flow. This is certainly true for an unbounded flow.

However if the interval in  $y$  is restricted to (say)

$-1 \leq y \leq 1$ , then it is necessary that

$$\sqrt{F_1 + 2r^2} < 2r^2$$

for  $y_c$  to be in the interval. This is true for sharp jets ( $r^2$  large) but not for diffuse jets ( $r^2$  small) so that sharp gaussian jets will be baroclinically unstable but it is not necessarily true for diffuse jets since they satisfy a necessary but not sufficient condition for instability.

#### Acknowledgment

It is a pleasure to acknowledge Melvin Stern for his many helpful criticisms.

#### References

- (1) Lin, C.C. (1955) Theory of Hydrodynamic Stability Cambridge University Press, Chapter 8: 121-123.

Experiments in Thermal Convection

by

Hans Thomas Rossby

## Experiments in Thermal Convection

Hans Thomas Rossby

### Introduction

A fluid contained between two infinite horizontal conducting planes is capable of transporting larger quantities of heat by convection than by conduction alone. Theoretical analysis shows that the heat transport is a function of two non-dimensional parameters, the Rayleigh number and the Prandtl number. There is however some confusion about the importance of the latter. Two theories have been developed for the fully turbulent convection. One, the Malkus theory, says that the Nusselt number,  $H/H_0$ , is independent of the Prandtl number,  $\sigma$ . The other approach is a mixing length analysis by R. Kraichnan in which he distinguishes between low and high  $\sigma$ . For high  $\sigma > 0.1$ , the Nusselt number is independent of  $\sigma$ , but for  $\sigma < 0.1$  it is proportional to  $\sigma^{-1/3}$ . For large Rayleigh numbers there is close agreement between the two as long as  $\sigma > 0.1$ . The large scatter of experimental data allows no critical examination.

This paper discusses the results of some experiments that were done in an attempt to get a better picture of this Prandtl number influence on the heat transport both at very low Ra (laminar convection) and high Ra (turbulent convection). The results are compared with two other experimental papers.

The experimental method.

The experimental apparatus is, with slight changes, a new model of the one used earlier by Malkus (1953). The fluid is contained between two aluminum plates by a surrounding plastic ring, which is also used for the vertical spacing. Next to each of the plates a large aluminum block is glued with a thin formica sheet in between. See fig. 1. When the lower block is heated and the upper cooled symmetrically around room temperature, they will act as heat capacities and the difference in temperature will set up a flow of heat through the fluid. Close to both sides of the formica plates are four thermocouples of copper-constantan. These are electrically isolated from the plates, but by filling the drill holes with mercury they are in good thermal contact. All the constantan leads are connected and by correct switching one can measure the temperature difference across the fluid,  $T_3 - T_2$ , or between the blocks  $T_4 - T_1$ .

Assuming that the system is in a steady state, one can very quickly compute the heat flow if the conductivity of the formica plates is known. This is an important advantage, that is to say, the effective conductivity is known simply by comparing the temperature across the fluid and the formica plates. (In most earlier experiments the heat transport has been measured by the electric energy input in a heating coil.) However, in this case, the blocks are slowly changing their temperatures due to the heat flow and the steady state is never completely achieved. The basic condition is therefore that the logarithmic

rate of decay must be small compared to the characteristic thermal diffusion time of the system. Because of the slight time-dependency it becomes necessary to establish how much the heat capacity of the aluminum and formica plates, as well as that of the fluid, can change the steady state estimate of the heat flow. In order to do this we assume the distance between the boundary plates is  $d$  and that the heat capacities per sq.cm. of the fluid, aluminum and formica plates are  $(d \rho C)_L$ ,  $(\ell \rho C)_{Al}$  and  $(\ell \rho C)_F$ . The vertical coordinate is  $z$  and the lower surface is  $z = 0$ , the upper  $z = d$ .

The one-dimensional heat equation is

$$\rho C \frac{\partial T}{\partial t} = -k \frac{\partial^2 T}{\partial z^2} \quad (1)$$

We assume that in a quasi-steady state the left side can be written:

$$\rho C \frac{\partial}{\partial t} T(z,t) = \rho C \frac{\partial}{\partial t} \left[ \left(1 - \frac{z}{d}\right) T_3(t) + \frac{z}{d} T_2(t) \right] \quad (2)$$

(2) in (1) and integrating in  $z$  gives:

$$-k \left( \frac{\partial T}{\partial z} \right)_{z=d} = -k \left( \frac{\partial T}{\partial z} \right)_{z=0} + \rho C z \frac{\partial T_3}{\partial t} - \rho C \frac{z^2}{2d} \frac{\partial}{\partial t} (T_3 - T_2) \quad (3)$$

Integrate once again from  $z = 0$  to  $z = d$  and divide by  $d$ :

$$-k \left( \frac{T_2 - T_3}{d} \right) = -k \left( \frac{\partial T}{\partial z} \right)_{z=0} + \rho C \frac{d}{2} \frac{\partial T_3}{\partial t} - \rho C \frac{d}{6} \frac{\partial}{\partial t} (T_3 - T_2) \quad (4)$$

For  $z = d$  we have from (3)

$$-k \left( \frac{\partial T}{\partial z} \right)_{z=d} = -k \left( \frac{\partial T}{\partial z} \right)_{z=0} + \rho C \frac{d}{2} \frac{\partial}{\partial t} (T_3 + T_2) \quad (5)$$

(4) rewritten:

$$-k \left( \frac{\partial T}{\partial z} \right)_{z=0} = k \frac{(T_3 - T_2)}{d} - \rho C \frac{d}{2} \frac{\partial T_3}{\partial t} + \rho C \frac{d}{6} \frac{\partial}{\partial t} (T_3 - T_2) \quad (6)$$

(4) and (5) give:

$$-k \left( \frac{\partial T}{\partial z} \right)_{z=d} = k \left( \frac{T_3 - T_2}{d} \right) + \rho C \frac{d}{2} \frac{\partial T_2}{\partial t} + \rho C \frac{d}{6} \frac{\partial}{\partial t} (T_3 - T_2) \quad (7)$$

Add (6) and (7):

$$-k \left[ \left( \frac{\partial T}{\partial z} \right)_{z=0} + \left( \frac{\partial T}{\partial z} \right)_{z=d} \right] = 2k \frac{(T_3 - T_2)}{d} - \rho C \cdot \frac{d}{6} \cdot \frac{\partial}{\partial t} (T_3 - T_2) \quad (8)$$

Assuming that there are no gradients in the aluminum plates,  
we have:

$$(\rho C l)_{Al} \frac{\partial T_2}{\partial t} = -k \left( \frac{\partial T}{\partial z} \right)_{z=d} + k_F \left( \frac{\partial T}{\partial z} \right)_{z=d+l_{Al}} \quad (9)$$

$$(\rho C l)_{Al} \frac{\partial T_3}{\partial t} = k \left( \frac{\partial T}{\partial z} \right)_{z=0} - k_F \left( \frac{\partial T}{\partial z} \right)_{z=-l_{Al}} \quad (10)$$

Subtract (9) from (10):

$$(\rho C l)_{Al} \frac{\partial}{\partial t} (T_3 - T_2) = k \left[ \left( \frac{\partial T}{\partial z} \right)_{z=0} + \left( \frac{\partial T}{\partial z} \right)_{z=d} \right] - k_F \left( \frac{\partial T}{\partial z} \right)_{z=-l_{Al}} - k_F \left( \frac{\partial T}{\partial z} \right)_{z=d+l_{Al}} \quad (11)$$

Using (8) and the equivalents of (6) and (7) for the two last terms of (11) we have:

$$\begin{aligned}
 (\rho C l)_{Al} \frac{\partial}{\partial t} (T_3 - T_2) &= -2k \frac{(T_3 - T_2)}{d} + \rho C \frac{d}{6} \frac{\partial}{\partial t} (T_3 - T_2) + \\
 + \frac{k_F}{2l_F} [(T_4 - T_1) - (T_3 - T_2)] &+ \frac{1}{2} (\rho C l)_F \frac{\partial T_3}{\partial t} + \frac{1}{6} (\rho C l)_F \frac{\partial}{\partial t} \left[ \frac{1}{2} (T_4 - T_1) - (T_3 - T_2) \right] + \\
 + \frac{k_F}{2l_F} [(T_4 - T_1) - (T_3 - T_2)] &- \frac{1}{2} (\rho C l)_F \frac{\partial T_2}{\partial t} + \frac{1}{6} (\rho C l)_F \frac{\partial}{\partial t} \left[ \frac{1}{2} (T_4 - T_1) - (T_3 - T_2) \right] \dots (12)
 \end{aligned}$$

The heat flow is then

$$H = k \frac{(T_3 - T_2)}{d} = \frac{k_F}{2l_F} \left\{ (\Delta_B T - \Delta T) - A \frac{\partial}{\partial t} (\Delta T) + B \frac{\partial}{\partial t} (\Delta_B T + 2 \Delta T) \right\} \quad (13)$$

where

$$A = \frac{l_F}{k_F} \left( (\rho C l)_{Al} - \frac{\rho C d}{6 Nu} \right)$$

$$B = \frac{l_F}{k_F} \cdot \frac{1}{6} \cdot (\rho C)_F$$

$$\Delta_B T = T_4 - T_1 \quad \Delta T = T_3 - T_2$$

The effective heat capacity of the fluid is the total capacity divided by the Nusselt number, hence the factor Nu in A. This formulation gives the average of the heat flow in and out of the fluid. If the system is changing its mean temperature very slowly, due to some asymmetric heat loss, its effect on H will be cancelled out.

As aluminum is only 25 times as conductive as mercury, it is necessary to make corrections for gradients that are present in the boundary plates when the latter is used.

If the steady state heat flow can be written

$$H_{s.s.} = \frac{(\Delta T)_e}{d} \cdot k_{eff} = \frac{(\Delta T)_{Al}}{d_{Al}} \cdot k_{Al} \quad (14)$$

and

$$(\Delta T)_e + (\Delta T)_{Al} = (\Delta T) \quad (15)$$

$$(\Delta T) = \text{measured } T_3 - T_2$$

$$(\Delta T)_e = \text{temperature drop across fluid}$$

$$(\Delta T)_{Al} = \text{temperature drop across aluminum}$$

We get:

$$(\Delta T)_e = \frac{\Delta T}{1 + \left(\frac{k_{eff}}{d}\right) \cdot \left(\frac{d}{k}\right)_{Al}} \quad (16)$$

This never involves more than a 4% correction and within limits of error the ratio  $k_{eff}/d$  can be considered as constant for

$$k_{eff}/k_{cond.} = Nu \sim Ra^{1/3} \sim d \text{ (turbulent convection).}$$

The electric system consists of a Keithley microvolt ammeter to which a Leeds-Northrup recorder is connected. The accuracy of the microvolt meter is  $\pm 2\%$  of full scale, which is a little large when switching ranges and the scales do not overlap. The linearity of the recorder was kept to better than 1%.

It is not obvious that at any arbitrary moment during the thermal decay, the system is a true representation of the steady state convection. However, if there is some unspecified hysteresis during the decay, it should have the opposite effect if the temperature across the fluid is increased instead. Assuming that this would be a good test of the validity of our results the following was attempted. Two additional cylindrical aluminum blocks were added to the original system, one heated and the other cooled. By having formica plates sandwiched at the surfaces of contact, one can regulate the heat flow and the rate of change in temperature across the fluid. Since it is difficult to heat and cool exactly symmetrically and add the blocks at exactly the same time, the original system is started in a reverse state, e.g., with  $T_1 > T_4$ . Then, hopefully, by the time  $T_3 > T_2$  the total system will have found a symmetric temperature distribution, if the added formica plates have exactly the same effective conductivity. The results are discussed later.

#### Laminar convection

The three fluids and their physical properties are given in Table #1.

Table #1. (at 25°C)

	Mercury	1.5 cs. Sil.oil.	1000 cs. Sil.oil.	Aluminum	Dim.
$\sigma$	.0257	18	8500		-
$\nu$	.001126	.015	10		$\text{cm}^2 \text{sec}^{-1}$
$\gamma$	.0438	.000847	.00118	.8	$\text{cm}^2 \text{sec}^{-1}$
$k$	.0197	.00025	.00038	$\sim .5$	$\text{cal cm}^{-2} \text{sec}^{-1} (\text{T} \cdot \text{cm}^{-1})^{-1}$
$\rho$	13.54	.853	.972	2.70	$\text{g} \cdot \text{cm}^{-3}$
$C$	.0332	.346	.332	.215	$\text{cal g}^{-1} \text{T}^{-1}$
$\alpha$	$.1818 \cdot 10^{-3}$	.00134	.00096		$\text{T}^{-1}$
$\frac{1}{\chi}$	23.	1200	850	1.25	$\text{sec cm}^{-2}$
$\frac{\alpha g}{\chi \nu}$	3630	10340	80		$\text{d}^{-3} \text{T}^{-1}$

Mercury has a very low Prandtl number and its physical properties do not change very much with temperature. The region around and above the critical Rayleigh number was studied for two geometries  $d = 1, 2$  cm, see fig. 2.\* The scatter in the apparent  $Ra_c$  for different runs was small and was not studied.

d(cm)	$\Delta T(Ra_c)$	Initial Slope		Sec. slope	Sec.Sl.Intersec. with Cond.Slope	Max.rate of decay	$\frac{\chi}{d^2}$
		min.	max.				
1	.475°C	1.07	1.16	1.46	$R = 2360$	<.04%	.044
2	.059°C	1.03	1.12	1.42	$R = 2610$	<.02%	.011

\*

Observe that the axes are reversed.  $Nu Ra$  can be called the normalized heat flow and is plotted as a function of  $Ra$ .

The recorded temperatures were corrected and re-plotted on a log temperature vs. time curve. This compression makes it easier to smooth out the wiggles in the data due to the limited conductivity of the aluminum. In spite of the large scatter from the wiggles, the agreement is satisfactory. The intersection of the second slope with the conduction line is not so well defined, but they overlap within  $\pm 5\%$  which is less than the maximum variation due to the wiggles. The character of the wiggles is different in the two slopes. In the second, they are very roughly periodic of 1-2 min. length, whereas in the first they become several min. long and aperiodic suggesting a slow final readjustment to a linear temperature profile in the fluid as it approaches the critical Rayleigh number during the decay.\*

Several attempts to increase the temperature, as described earlier, were done and the most successful one has a few points plotted in fig. 2,

They do not lie on the line because the rate of increase is too large for the system to readjust itself. As soon as the rate of change becomes small, then all points lie within the limits indicated and during the rest of that run there was no distinguishable hysteresis. Because of the difficulties and lack of time this technique was not repeated.

The initial slopes for the two silicone oils were also studied, but lack of time did not allow any repeat runs to check consistency. Contrary to the studies with mercury, the time corrections involved

---

\*The time constant for the electric system is  $< 2$  sec.

for computing the heat flux became very large (10-15%). Another very important correction was due to the heat transport parallel with the fluid through the container wall. To simplify the data processing the conductive slope was computed from the handbook value. The difference in the conductive slopes was assumed completely attributable to the transport through the wall and proportional to  $T_3 - T_2$ . The slope, 2.58, agrees very well with earlier experimental data (Silveston). Strangely, the critical transition did not occur at the computed critical temperature, but at  $\sim 50\%$  higher  $T_3 - T_2$ . The physical properties, specially the viscosity, were checked and agreed with handbook values. Dr. Melvin Stern suggested that the fluid might be contaminated by some minute foreign particles which by stratification could have a stabilizing effect. This would not necessarily affect the initial slopes.

The initial slope for the 1000 cs. fluid is less, 2.23, but it is not reliable for the rate of decay was .02% or less and  $\frac{\kappa}{d^2} = .0003$ , which are comparable.

	d	$(\Delta T)Ra_c$	Slope*	"Transient Slope"	Rate of Decay	$\frac{\kappa}{d^2}$
1.5cs	.5cm	0.2°C	2.58		<.03%	.0035
10 <sup>3</sup> cs	2.cm	2.66°C	2.23	1.92	<.02%	.0003

\*It is not possible to give limits of error of physical significance, but  $\pm 5\%$  is a conservative estimate of the experimental errors if the corrections are correct.

In both cases there is a "transition" slope. See fig. 3,4. This has been observed by Malkus in his earlier experiments, but Silveston does not mention it although his data does scatter somewhat in a similar way. It would be particularly advantageous to go through this transition while increasing the temperature to check its consistency.

#### Turbulent Convection

Mercury was studied extensively for high Ra under varying constraints. Two runs were done with  $d = 4$  cm, one with  $d = 8$  cm, and one at  $d = 4$  cm, but with a plastic divider that sectioned the fluid into four vertical compartments. In fig. 4,  $NuRa$  is plotted against Ra. It is clear that as the ratio  $d$  to  $\ell$  (diameter!) is increased the heat transport becomes larger. This is very interesting showing how a simple geometric constraint on the fluid will give rise to an increase in the heat transport. The best values are for  $d = 4$  cm without the divider. The original data was smoothed on a logarithmic plot. Then the heat transport was plotted against the Ra on a linear diagram. Corrections were made for gradients in the plates and the Nusselt number was computed at various Ra numbers. These were plotted to give fig.5. It is not quite clear why the slope is not  $4/3$  as it should be. Probably as Ra decreased, the effects from the poor geometry of the system became more significant. The line from Globe & Dropkin is plotted for comparison. For these Ra their geometry  $d/\ell$  was 0.26 which is somewhat better than here,

0.4. As the best data scatters around their line, but still shows a trend towards smaller Nu, it is possible that the coefficient in the line equation  $NuRa = 0.051 \cdot Ra^{4/3}$  is slightly large. Kraichnan's mixing-length analysis predicts the coefficient to be 0.048.

The results from the silicone oils are more difficult to interpret.

$\sigma$	d	Ra	Nu						Rate of Decay
			ours	Globe & Dropkin	Silveston	Mull & Reiher	Kraichnan	Malkus	
18	8	$24.2 \cdot 10^6$	21.5	28.4	-	-	25.7	22.9	<.02%
8500	8	$395 \cdot 10^3$	6.65	10.0	6.3	$\sim 6.3$	6.5	5.8	<.02%
8500	12	$1.14 \cdot 10^6$	8.9	14.0	-	$\sim 8.4$ (air) $\sigma=0.7$	9.3	8.3	<.02%

Unfortunately the corrections for the heat transport in the container walls were very large 20 to 30%. Since these values are from single runs it is not possible to specify the limits of error, but  $\pm 10\%$  for processing errors is certainly sufficient. How Globe and Dropkin get such large Nusselt numbers is not clear. They use one container with  $d/\ell = .4$  and heat the silicone oils to large temperatures where the fluids no longer are Boussinesq.

For the 1.5 cs. silicone oil,  $\sigma = 18$ , the Nusselt number is too low. It is possible that the ratio  $d/\ell$  is unfavorable. Or, it may be that the 50% difference between the computed and observed  $(Ra)_{crit}$  is significant. All this is speculation, but it might be added that Globe and Dropkin computed their Ra without making observations of  $Ra_{crit}$ .

Also they

Also, they did not discuss what corrections they had to make, for example, for losses from the heating unit or, more likely, for the heat conduction in the container wall. Unless the geometry of the fluid container was a very serious constraint on the turbulent convection it seems difficult to understand their high values. The values reported here seem to lie rather close to Kraichnan's computed values, but they cannot be considered as conclusive. It is nevertheless well established that there is a strong  $\sigma$  influence at low  $\sigma$  at both low and high Rayleigh numbers.

It is interesting, nevertheless, how the geometry of the container will affect the heat transport for low and high  $\sigma$ . As  $d/\ell$  increases, the characteristic size of convective "blobs" becomes smaller. For high  $\sigma$  this increases the viscous dissipation whereas at low  $\sigma$ , the viscous dissipation being less significant, the convection becomes more organized.

#### Acknowledgment

The author wishes to thank Prof. W.V.R.Malkus for his suggestion and his valuable support of these experiments.

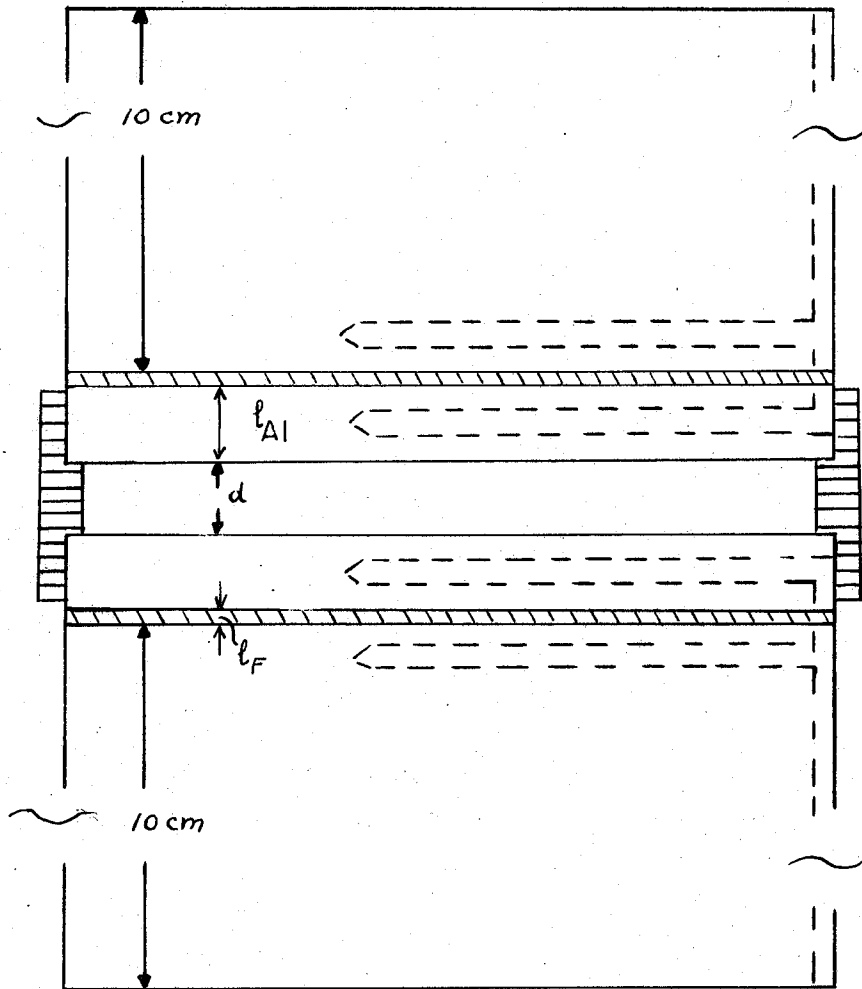
References

Malkus, W.V.R., Proc.Roy.Soc.London A 225, 185 (1954).

Silveston, P.L., Forsch.Ing. - Wes. Bd. 26, 29-32, 59-69 (1958).

Globe, S. and D. Dropkin, Trans.Am.Soc.Mech.Engrs., J.Heat Transfer, 81, 24 (1959).

Kraichnan, R.H., Research Report No. HSN-6, N.Y.U. (1962).



Scale 1:1

-  plastic
-  formica
-  aluminum

FIGURE 1.

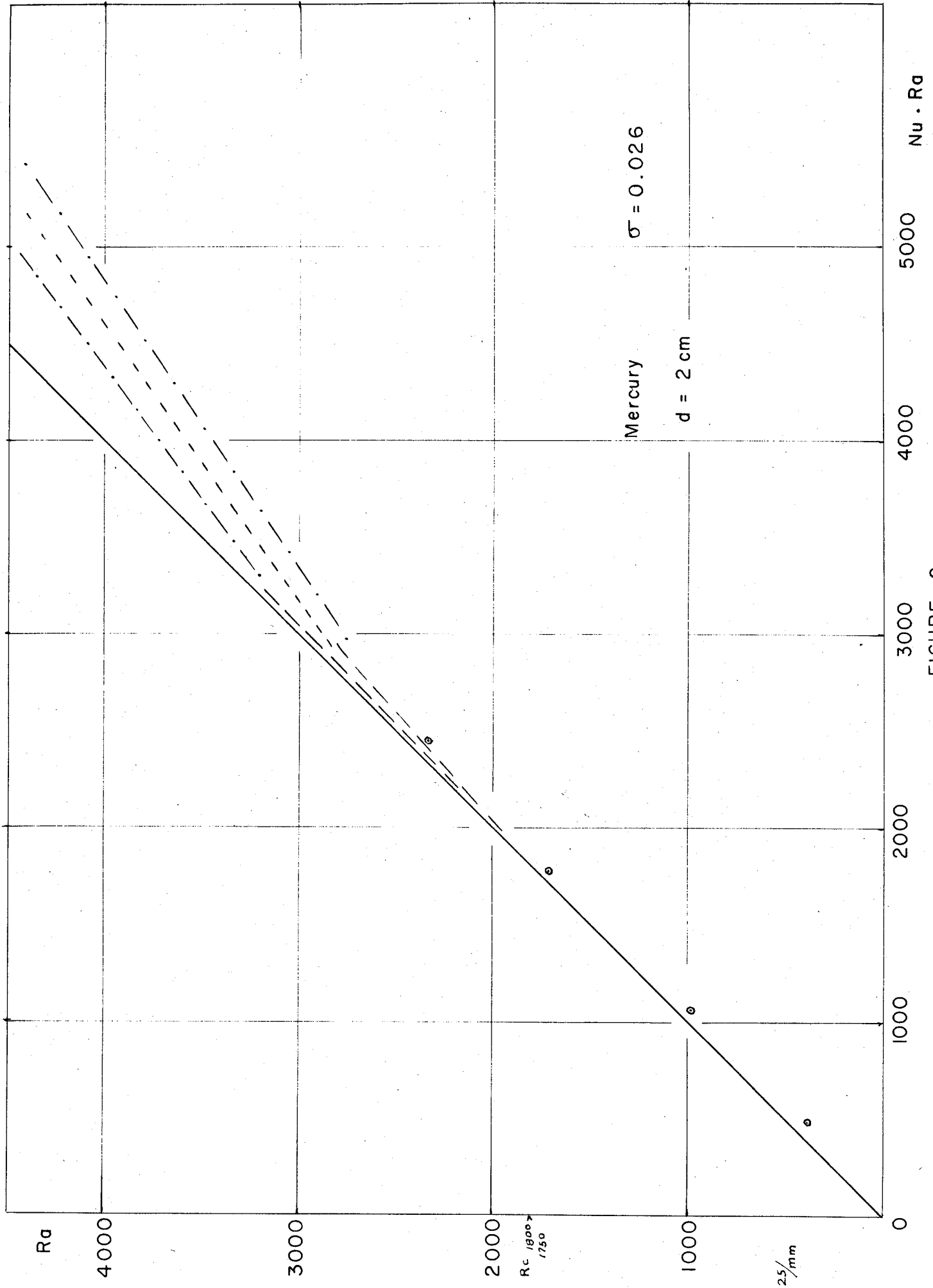


FIGURE 2

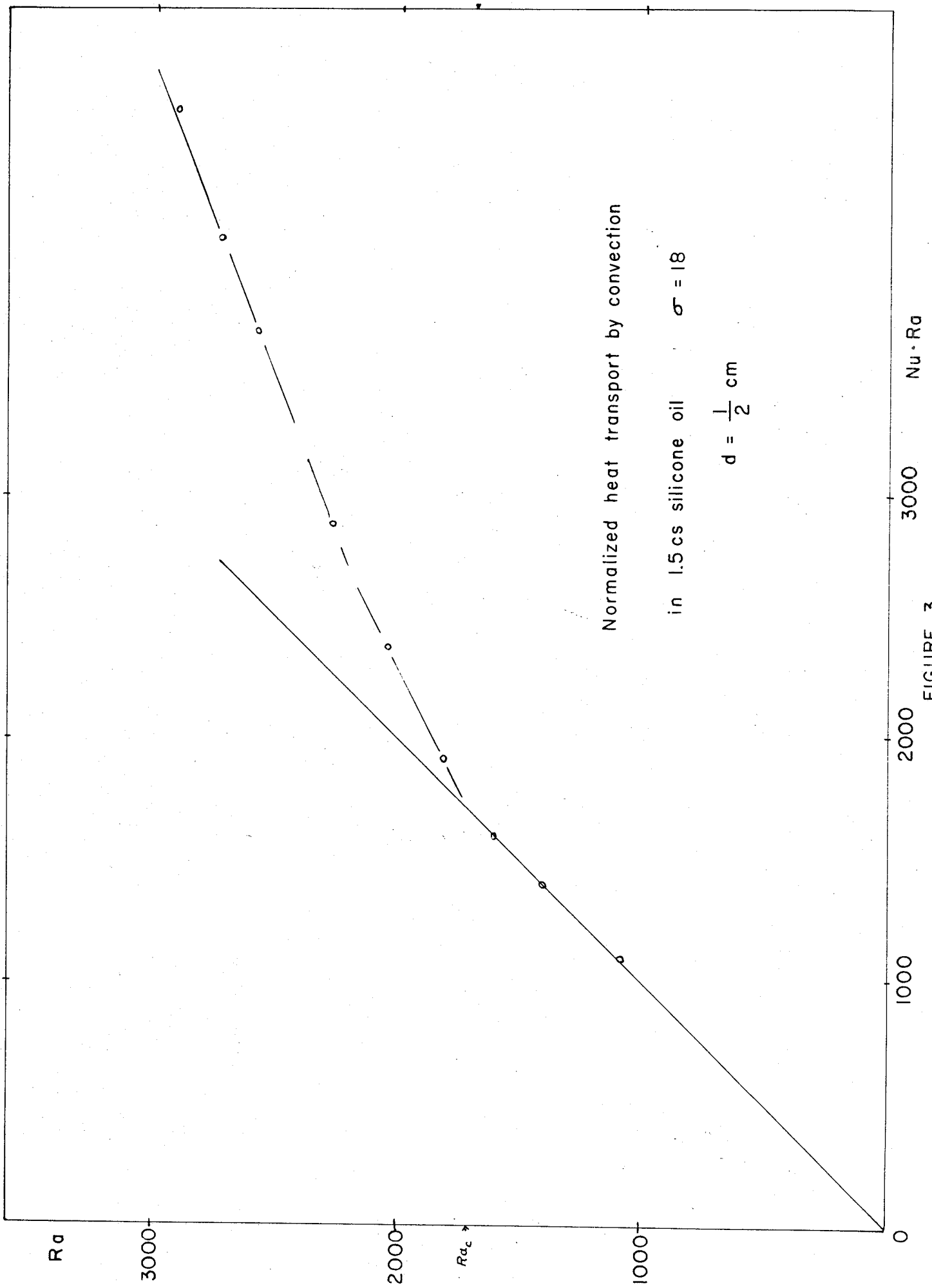


FIGURE 3

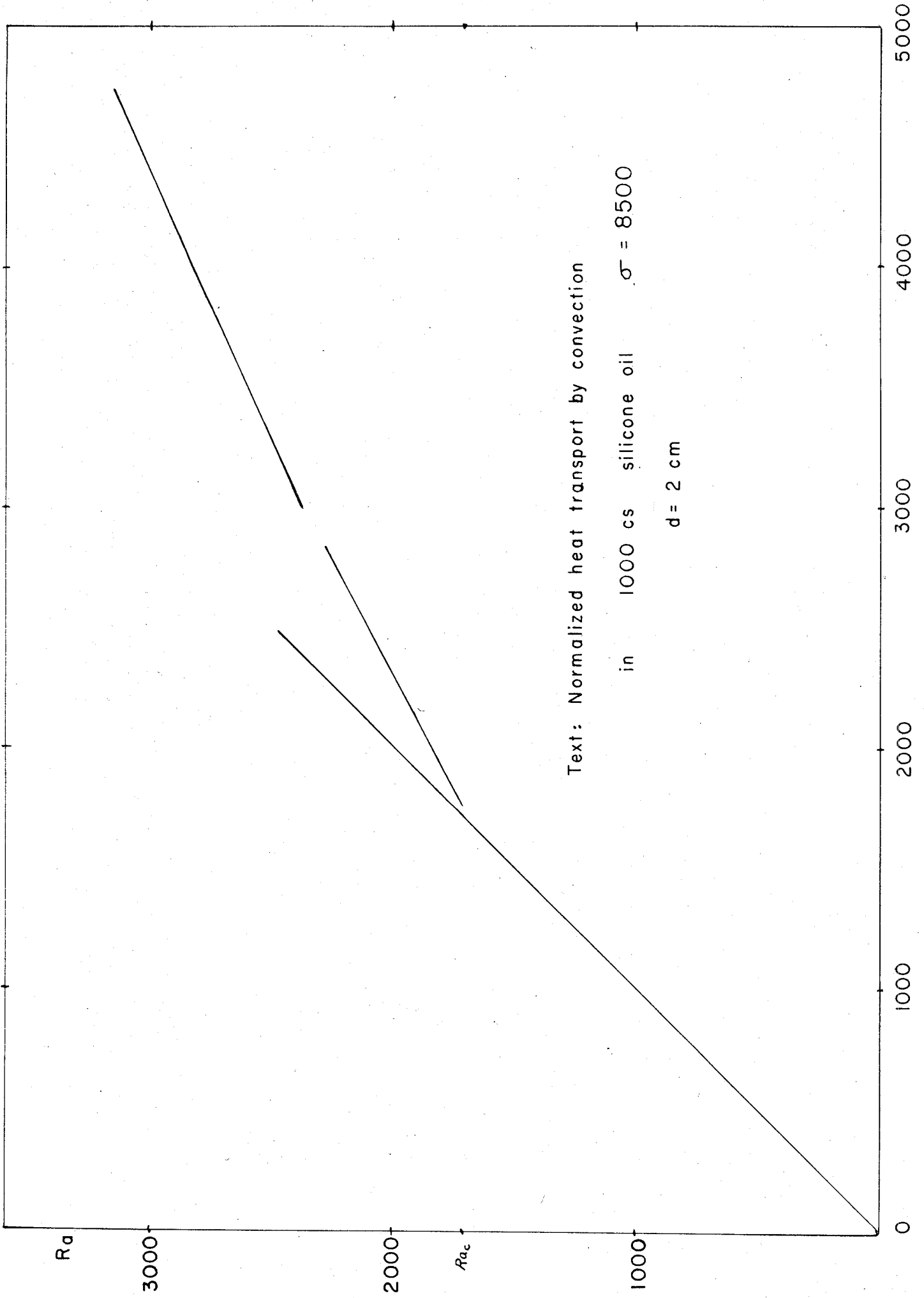


FIGURE 4

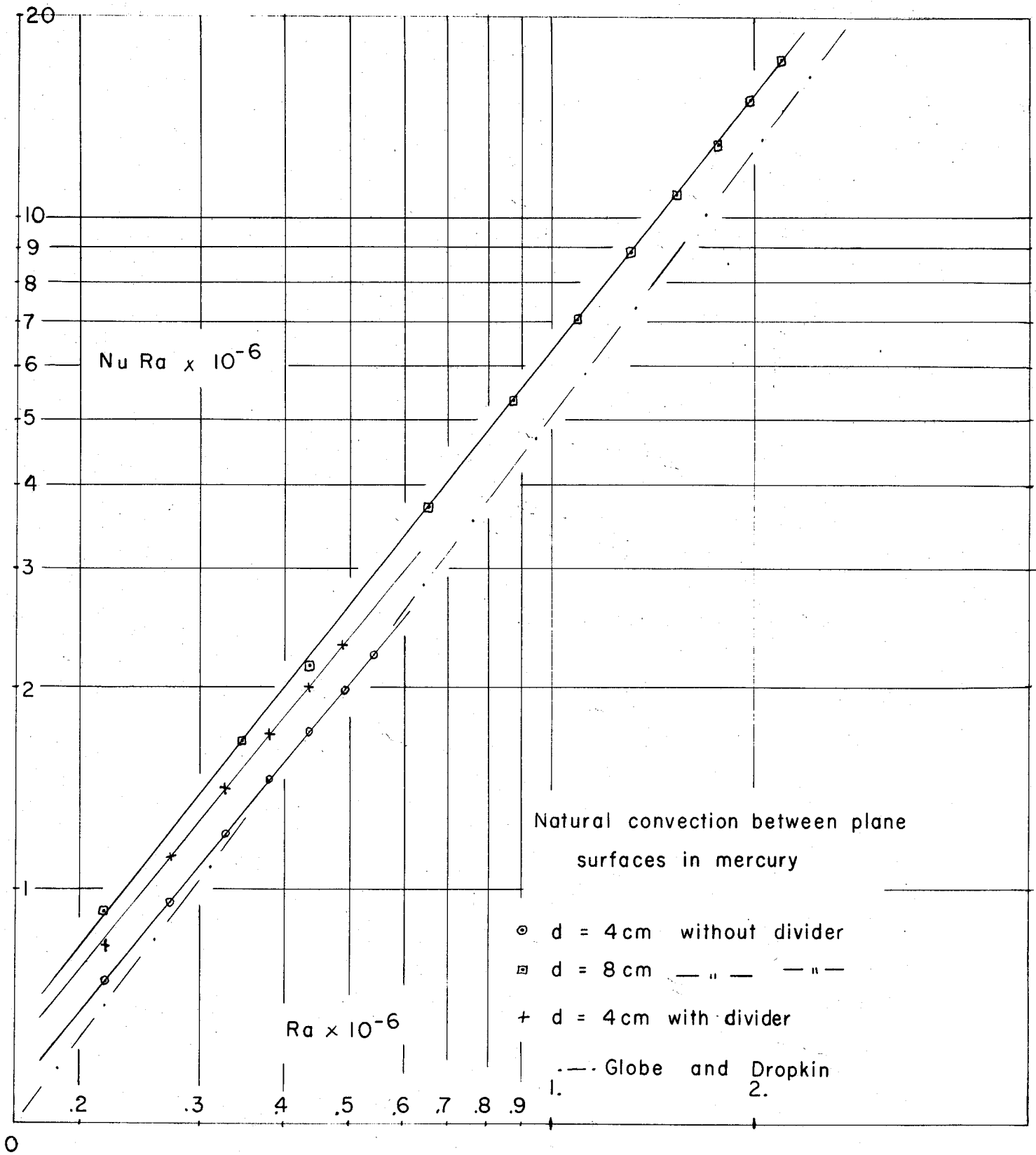


FIGURE 5

**On the Problem of Finite Amplitude Convection**

by

**P. Souffrin**

## On the Problem of Finite Amplitude Convection

P. Souffrin, IAP

**Summary:** A rapid review is given of different methods that can apply to the study of finite amplitude convection.

The situation under consideration is the so-called "thermal instability". Roughly speaking, it is the instability illustrated by a fluid heated from below. Due to the fact that the fluid expands when heated, the situation is gravitationally unstable. Viscosity may inhibit the onset of the motion, but clearly if a sufficient upward gradient is maintained between two horizontal layers of a fluid, some steady or statistically steady state of motion will be reached. That this motion results in a "convective" heat flux is understandable from the fact that, due to the very nature of the instability, the average temperature of the fluid moving upwards is higher than the average temperature of the fluid moving downwards.

In most theoretical or experimental studies, fluids are considered which are everywhere either stable or unstable, though in nature the convection is generally "penetrative", i.e. the average horizontal structure is thermally unstable only in a limited part of the fluid. As the motion cannot be strictly confined in the "unstable" part of the fluid, the convection is said to "penetrate"

in the "stable" fluid. The argument referred to above as to the direction of the convective heat transport is not relevant for the motion in the stable region which may transport heat downwards. This is suggested by extrapolating to the stable region the mixing length theory estimation of the convective heat flux. This extrapolation is of course questionable, but the idea receives some support from a recent study of penetrative convection by Dr. George Veronis. In the situation considered by Veronis, the fundamental mode of steady motion does not transport heat in the same direction through the entire volume of the fluid.

In any case, the knowledge of the convective conductivity is the main problem related to thermal instability, besides the extensively-studied conditions of stability. This knowledge can only be obtained through the consideration of the non-linear coupling between the different modes of motion. Though this problem is generally attacked by introduction of phenomenological assumptions, a more direct approach has been developed by Malkus and Veronis (1958). Following Malkus and Veronis, we will sketch different ways to obtain formal solutions of the system of non-linear equations describing the finite amplitude convection in the Boussinesq approximation.

To illustrate the procedure, we will consider instead of the exact system of relevant equations, the following system:

$$I \quad \left\{ \begin{array}{l} (\nabla^6 - \lambda \nabla_{\perp}^2) W = F_3(W, W, W) - \frac{1}{\sigma} F_2(W, W) \\ + \text{boundary conditions at } g = 0 \text{ and } z = 1. \end{array} \right.$$

where

$$\nabla^2 \equiv \frac{\partial^2}{\partial x^2} + \frac{\partial^2}{\partial y^2} + \frac{\partial^2}{\partial z^2}$$

$$\nabla_{\perp}^2 \equiv \frac{\partial^2}{\partial x^2} + \frac{\partial^2}{\partial y^2}$$

$\lambda$  and  $\sigma$  are scalar parameters

$F_2$  and  $F_3$  are homogeneous functions of order 2 and 3 in  $W$  and the derivatives of  $W$ .

The linear part of system I is identical to the linearized equation for the vertical component of the velocity of the Boussinesq system, if  $\lambda$  is the Rayleigh number and  $z$  the vertical coordinate. The non-linear part is somehow suggestive of the way the Prandtl number occurs in the Boussinesq system, if  $\sigma$  represents the Prandtl number. As regards to the horizontal boundary conditions, we will restrict to cellular-like patterns of given horizontal wave number  $\alpha$ . The eigen functions of the linear system are then separable, and the set of eigen values is discrete. We have

$$(1) \quad (\nabla^6 - \lambda_{pq} \nabla_{\perp}^2) \varphi_{pq} = 0$$

where

$$(2) \quad \begin{cases} \varphi_{pq} = X_p(z) \psi_q(x, y) \\ \nabla_1^2 \psi_q = -(q\alpha)^2 \psi_q(x, y) \end{cases}$$

$p$  and  $q$  being any non-zero positive integers.

The lowest eigen value, i.e.  $\lambda_{11}$ , is the critical Rayleigh number associated with  $\alpha$ . We will admit that the  $\varphi_{pq}$  provide a complete set of functions compatible with the boundary conditions.

The solution of I cannot be obtained explicitly, but clearly in the vicinity of marginal stability, i.e. for  $\lambda \simeq \lambda_{11}$ , the amplitude of  $W$  will be small (disregarding the possibility of finite amplitude disturbances). The system I then becomes quasi-linear, a situation well known in celestial mechanics. A procedure then consists in expanding formally  $W$  in powers of some function  $\epsilon$  of the small parameter, splitting the system into an infinite number of linear non-homogeneous systems. These systems generally have no solutions (i.e. no solutions compatible with the boundary conditions) but the procedure introduces arbitrary constants: constants of integrations, and constants involved in the definition of  $\epsilon$ . Different choices of these constants can be made so that all the systems have solutions.

Let us write I

$$S \quad \begin{cases} (\nabla^6 - \lambda_{11} \nabla_1^2) W = \delta \lambda W + F_3 - \frac{1}{\sigma} F_2 = \mathcal{F}(W). \\ + \text{boundary conditions} \end{cases}$$

where  $\delta\lambda = \lambda - \lambda_0$  is to be considered as small, and is in fact the small parameter of physical interest. The parameter of the expansion will be some function of  $\delta\lambda$ , and it is convenient to write the relationship under the form

$$(3) \quad \delta\lambda = \delta\lambda(\epsilon) = \bar{\omega}_1 \epsilon + \bar{\omega}_2 \epsilon^2 + \bar{\omega}_3 \epsilon^3 + \dots$$

the  $\bar{\omega}_i$  being coefficients to be defined.

Writing

$$(4) \quad W = W_1 \epsilon + W_2 \epsilon^2 + W_3 \epsilon^3 + W_4 \epsilon^4 + \dots$$

in  $\mathcal{D}$ , and equating to zero all the powers of  $\epsilon$ , one gets the systems

$$S_m \begin{cases} (\nabla^6 - \lambda_0 \nabla^4) W_m = \mathcal{F}_m(W_{m-1}, W_{m-2}, \dots, W_1) \\ + \text{boundary conditions} \end{cases}$$

where

$$(5) \quad \mathcal{F}_m = \sum_{i+j=n} [\bar{\omega}_i W_j - \frac{1}{\sigma} F_2(W_i, W_j)] + \sum_{i+j+k=n} F_3(W_i, W_j, W_k)$$

$$\sum_{i+j=n} = \sum_{i=1}^n \sum_{j=1}^{n-i}$$

Since  $\mathcal{F}_m$  depends only on  $W_p$  and  $\bar{\omega}_q$  for  $p, q < n$ ,  $S_m$  is a linear

homogeneous system depending on the solutions for  $S_p$  for  $p < n$ . For  $S_n$  to have a solution it is clearly necessary that  $F_n$  be orthogonal to  $\varphi_{11}$ , that is:

$$(6) \quad \int dr_0 \tilde{\varphi}_{11}(r_0) F_n \{W(r_0)\} = 0.$$

$\tilde{\varphi}$  being the conjugate of  $\varphi$ .

If (6) is verified, then

$$(7) \quad W_n = C_n \varphi_{11} + \int dr_0 G(r/n_0) F_n$$

is solution of  $S_n$ , where  $C_n$  is an arbitrary constant of integration and where the Green's function  $G(r/n_0)$  is readily seen to be

$$(8) \quad G(r/n_0) = \sum_{p \neq 1, q \neq 1} \frac{\tilde{\varphi}_{pq}(r_0) \varphi_{pq}(r)}{(q\alpha)^2 (\lambda - \lambda_{pq})}$$

Eq. (6) is then a necessary and sufficient condition for  $S_n$  to have a solution. Once  $W_p$  is found for  $1 \leq p \leq n$ , the two constants  $C_n$  and  $\bar{w}_n$  can be chosen so that  $S_{n+1}$  has a solution. Malkus and Veronis choose  $C_1 = 1$ ,  $C_p = 0$  for  $p \neq 0$ , and can then determine the  $\bar{w}_1$  from (5) and (6). With a standard notation, they have:

$$\bar{w}_m \langle \varphi_{11} | W_1 \rangle = - \sum_{i+j=m} \bar{w}_i \langle \varphi_{11} | W_j \rangle + \frac{1}{\sigma} \sum_{i+j=n+1} \langle \varphi_{11} | F_2 \rangle - \sum_{i+j+k=n+1} \langle \varphi_{11} | F_3 \rangle$$

Other choices of the  $C_m$  are possible which lead to other expansions. For instance, for the Rayleigh Boussinesq problem with free-free

boundary conditions, it turns out that one can determine the  $C_n$  with the requirement  $\bar{w}_n = 0$  for  $n \neq 2$  and  $\bar{w}_2 = 1$ .  $W$  is then an expansion in powers of  $(\delta\lambda)^{\frac{1}{2}}$ :

$$(9) \quad W = W_1(\delta\lambda)^{\frac{1}{2}} + W_2(\delta\lambda) + W_3(\delta\lambda)^{\frac{3}{2}} + \dots$$

No estimation of the radius of convergence of the possible expansion has yet been found. But comparing the results can provide some information, the different expansions being equivalent if convergent in some vicinity of  $\delta\lambda = 0$ .

A more direct method can be developed writing  $S$  into the equivalent form

$$S^* \begin{cases} W(n) = C \varphi_n + \int d\underline{n}_0 G(n/n_0) \mathcal{F}\{W(n_0)\} \\ + \text{boundary conditions} \end{cases}$$

$C$  being a constant determined by the boundary conditions. One can substitute into the boundary conditions the equation:

$$\langle \varphi_{||} | \mathcal{F}(W) \rangle = 0$$

so that  $S^*$  can be written:

$$S^{**} \begin{cases} W(n) = C \varphi_{||} + \int d\underline{n}_0 G(n/n_0) \mathcal{F}(W(n_0)) \\ \int d\underline{n}_0 \tilde{\varphi}_{||} \mathcal{F}(W) = 0 \end{cases}$$

$S^{**}$  can be iterated in a straightforward way:

$$S_0^{**} : W_0 = C_0 \varphi_{11}$$

$$S_1^{**} \begin{cases} W_1 = C_1 \varphi_{11} + \int dr_0 G(r/r_0) \mathcal{F}(W_0) \\ \langle \varphi_{11} | \mathcal{F}(W_0) \rangle = 0 \end{cases}$$

---

$$S_n^{**} \begin{cases} W_n = C_n \varphi_{11} + \int dr_0 G(r/r_0) \mathcal{F}(W_{n-1}) \\ \langle \varphi_{11} | \mathcal{F}(W_{n-1}) \rangle = 0 \end{cases}$$

\* \* \*

The author intends to examine the coefficients introduced at each step and to compare the different methods of solution.

Finite Amplitude Evolution  
of Large Scale Atmospheric Disturbances

by

R. T. Williams

# Finite Amplitude Evolution of Large Scale Atmospheric Disturbances

R. T. Williams

## Introduction

Recently a number of studies have been made in which more complicated equations than the quasigeostrophic ones are employed (see, for example, Hinkelman (1959), who solved the hydrostatic primitive equations numerically). These studies have been stimulated in part by inadequacies in operational quasigeostrophic forecasts. In this paper some of the effects on the growth of an atmospheric disturbance, which are not included in the quasigeostrophic approximation, will be studied. These effects are essentially non-linear, and will be investigated with a finite amplitude expansion. To simplify the problem, only perturbations which have no latitudinal variation will be considered, and finite differences will be used in the vertical to construct a two-level model.

## Governing Equations

As indicated above we are only considering disturbances which have no northward variation. That is, the velocity components and the deviation from the zonal mean of the temperature and geopotential are taken as constant in latitude. Also, friction, heating, and the variation of the Coriolis parameter are neglected.

These restrictions on the flow have several important consequences. Since  $f$  (the Coriolis parameter) is constant, there can

be no Rossby waves, and the baroclinic stability criteria will be modified. No convergence of the poleward fluxes of heat and momentum can occur as these quantities do not vary with latitude. Thus, in this model the latitudinal temperature gradient must remain constant. In a bounded system a convergence of this poleward flux is expected, and this would reduce the poleward temperature gradient, and tend to stabilize the flow. The latitudinally constant momentum flux implies that no poleward variations in the zonal wind can develop, and therefore that horizontal barotropic instability cannot occur. The neglect of heating and friction in the model will be important when longer time periods are considered.

However, the constant  $f$  does not change the gross baroclinic stability relationships, and it does allow the unstable disturbances to have a simpler, more symmetric vertical structure. The exclusion of the flux convergence processes permits the isolation of other physical effects.

We shall employ the two-level model used by Eliassen (1956) and Smagorinsky (1958). In this model pressure is used as a vertical coordinate, and the atmosphere is divided into four layers of constant pressure differential  $\frac{1}{2} \Delta P$ . The bounding pressure levels are numbered from 0 to 4, where level 0 corresponds to the top of the atmosphere, where  $p = 0$ , and level 4 corresponds to the earth's surface where  $p = 2 \Delta P$ . Applying the equations of motion and the

continuity equation at levels 1 and 3, approximating vertical derivatives with finite differences, and combining, we obtain:

$$\frac{\partial u_1}{\partial t} + u_1 \frac{\partial u_1}{\partial x} + \frac{\partial u_1}{\partial x} \frac{(u_1 - u_3)}{2} = - \frac{\partial \phi_1}{\partial x} + f v_1, \quad (1)$$

$$\frac{\partial u_3}{\partial t} + u_3 \frac{\partial u_3}{\partial x} - \frac{\partial u_3}{\partial x} \frac{(u_1 - u_3)}{2} = - \frac{\partial \phi_3}{\partial x} + f v_3, \quad (2)$$

$$\frac{\partial v_1}{\partial t} + u_1 \frac{\partial v_1}{\partial x} + \frac{\partial u_1}{\partial x} \frac{(v_1 - v_3)}{2} = - \frac{\partial \phi_1}{\partial y} - f u_1, \quad (3)$$

$$\frac{\partial v_3}{\partial t} + u_3 \frac{\partial v_3}{\partial x} - \frac{\partial u_3}{\partial x} \frac{(v_1 - v_3)}{2} = - \frac{\partial \phi_3}{\partial y} - f u_3, \quad (4)$$

where  $\phi$  is the geopotential. Here the usual meteorological cartesian coordinates are employed, which means that the terms involving the inverse of the earth's radius have been neglected. The subscripts on the dependent variables indicate the appropriate pressure levels.

In this model the vertically averaged continuity equation takes the form:

$$\frac{\partial}{\partial x} (u_1 + u_3) = 0 \quad (5)$$

This implies that the vertical mean divergence is zero, and results from the assumption that the individual pressure change at the earth's surface vanishes. This is a good approximation for all but the planetary scale motions in the atmosphere. Also, this assumption filters external gravity waves out of the model.

If  $-\frac{\partial \phi_1}{\partial y} - \frac{\partial \phi_3}{\partial y} + f(u_1 + u_3)$  and  $(\bar{v}_1 + \bar{v}_3)$  are zero, then the time variation of  $u_1 + u_3$  must also vanish (the bar indicates the horizontal mean). We shall consider only such cases, and since the frame of reference is arbitrary we shall take:

$$u_1 + u_3 = 0. \quad (6)$$

When the thermodynamic energy equation is applied at level 2, and the hydrostatic equation and the continuity equation are employed, we obtain:

$$\frac{\partial}{\partial t} (\phi_1 - \phi_3) + \frac{(v_1 + v_3)}{2} \frac{\partial}{\partial y} (\phi_1 - \phi_3) + \frac{R \Delta P}{2 \kappa} \left( - \frac{\partial \theta}{\partial p} \right)_2 \frac{\partial u_1}{\partial x} = 0, \quad (7)$$

where

R = gas constant,

$\theta$  = potential temperature,

$C_p$  = specific heat at constant pressure,

$$\kappa = \frac{R}{C_p}.$$

The measure of the static stability in this model,  $\left( - \frac{\partial \theta}{\partial p} \right)_2$ , is taken as horizontally constant, but will be allowed to vary in time.

By horizontally averaging the equation:

$$\frac{\partial}{\partial p} \left( \frac{d\theta}{dt} \right) = 0$$

and applying finite differences an expression for this time variation may be found.

In order to separate out the mean fields, and simplify the

equations we introduce the following new variables:

$$u_1 = -u_3 = u + u_0(t) + u(x, t) \quad (9)$$

$$v = -\frac{1}{f} \frac{\partial \phi_1}{\partial y} = \frac{1}{f} \frac{\partial \phi_3}{\partial y} \quad (10)$$

$$\frac{1}{2}(v_1 - v_3) = v_m \quad (11)$$

$$\frac{1}{2}(v_1 - v_3) = v_0(t) + v_T(x, t) \quad (12)$$

$$\frac{1}{2}(\phi_1 - \phi_3) = \phi_T. \quad (13)$$

Now  $u$ ,  $v_m$ ,  $v_T$ , and  $\phi_T$  have zero horizontal averages.

Before rewriting the equations let us non-dimensionalize with the following relations:

$$x = \frac{x'}{R}, t = \frac{t'}{RU}, \phi = \frac{fU}{R} \phi', v = UV', u = \mu U u', v_0 = \mu^2 U v_0', u_0 = \mu U u_0'. \quad (14)$$

The Rossby number is  $\mu = \frac{RU}{f}$ , where  $R$  is a wave number for the flow. Another non-dimensional number is given by:

$$\gamma_0 = \frac{R \Delta P}{2^{1+\kappa}} \left( -\frac{\partial \Theta}{\partial p} \right) \frac{R^2}{f^2} - \mu \delta(t). \quad (15)$$

Thus,  $\gamma_0$  is the product of a Richardson's number and the Rossby number squared.

On introducing the new dependent variables and non-dimensionalizing, the system of equations may be written in the following form:

$$\frac{\partial v_m}{\partial t} + \frac{\partial v_T}{\partial x} = \mu \left[ -u_0 \frac{\partial v_T}{\partial x} - \frac{\partial}{\partial x} (u v_T) \right] \equiv M, \quad (16)$$

$$\frac{\partial v_T}{\partial t} + \frac{\partial v_m}{\partial x} + u = \mu \left[ -u_0 \frac{\partial v_m}{\partial x} - u \frac{\partial v_m}{\partial x} + \overline{u \frac{\partial v_m}{\partial x}} \right] \equiv N, \quad (17)$$

$$\mu^2 \frac{\partial u}{\partial t} + \frac{\partial \phi_T}{\partial x} - v_T = 0, \quad (18)$$

$$\frac{\partial \phi_T}{\partial t} - v_m + \gamma_0 \frac{\partial u}{\partial x} = -\mu \gamma \frac{\partial u}{\partial x} \equiv P, \quad (19)$$

$$\mu^2 \frac{d v_0}{dt} - u_0 = \mu \overline{\left( \frac{\partial u}{\partial x} v_m \right)} \equiv T, \quad (20)$$

$$\frac{d u_0}{dt} - v_0 = 0 \quad (21)$$

$$\frac{d Y}{dt} - 2 \mu^2 v_0 = -2 \mu \overline{\left[ u \frac{\partial \phi_T}{\partial x} \right]} \equiv Q, \quad (22)$$

where the primes have now been dropped. Notice that the left-hand sides of the above equations contain all the linear terms, and that the right-hand sides are non-linear, and are denoted by M, N, P, T, and Q, respectively.

With the scaling used in this analysis all quantities except  $\mu$  and  $\gamma_0$  should be of order one for large scale atmospheric flow. For such motion  $\mu$  is usually of order .1, and  $\gamma_0$  is one or less. If we neglect all terms of first and higher order in the Rossby number, we obtain the usual quasigeostrophic system of equations. Notice that the quasigeostrophic equations in this case are completely linear. A higher order approximation can be obtained by including the terms of first order in  $\mu$ . Such a formulation might be called a balanced system since it includes non-geostrophic effects, but does not allow gravitational-inertial motions. Note

that all the non-linear terms in the above system are of the first order in the Rossby number.

In discussing the physical meaning of the terms in the above equations, it is useful to note that since the  $y$  variation of the velocity is zero,  $u$  is the divergent part of the horizontal velocity, and  $v$  is the rotational part. Thus, the non-linear terms in equations (16) and (17) which do not involve  $u_0$ , represent the vertical advection, and the horizontal advection by the divergent part of the wind, of the rotational component of the velocity. As will be seen later, these terms cause an energy cascade which can drain kinetic energy from the energy-producing modes of the system. Such a process cannot occur with the quasi-geostrophic approximation, in this case, because the governing equations are linear. With two horizontal dimensions, a cascade may occur in the quasigeostrophic model, but as Phillips (1959) has pointed out, this energy transfer appears to be small. Thus, one of the major differences between the quasigeostrophic equations and the primitive equations, may lie in the rate of energy transfer to shorter wave lengths.

The terms involving  $u_0$  in equations (16) and (17) represent the advection by the non-geostrophic part of the zonal mean wind. In equation (19),  $P$  indicates the change in the vertical advection of potential temperature, due to a time variation in the static stability. The non-linear term in equation (20) shows the effect on the meridional circulation of a mean vertical flux of  $v$  momentum,

since  $\frac{\partial u}{\partial x}$  is proportional to the vertical velocity. In equation (22), the static stability varies according to the meridional circulation and the vertical heat flux.

### Solution Procedure

We will obtain approximate solutions to the above system of equations by using a finite amplitude expansion similar to that employed by Malkus and Veronis (1958). However, they sought steady state solutions, while we are interested in the time evolution.

For convenience, we obtain the following equation whose linear part contains only  $v_T$  :

$$\begin{aligned} \mathcal{L}(v_T) &\equiv \left[ \left( \mu^2 \frac{\partial^2}{\partial t^2} - \gamma_0 \frac{\partial^2}{\partial x^2} + 1 \right) \frac{\partial^2}{\partial t^2} - \left( \mu^2 \frac{\partial^2}{\partial t^2} - \gamma_0 \frac{\partial^2}{\partial x^2} - 1 \right) \frac{\partial^2}{\partial x^2} \right] v_T \\ &= L \equiv \frac{\partial^2 P}{\partial x \partial t} + \left( \mu^2 \frac{\partial^2}{\partial t^2} - \gamma_0 \frac{\partial^2}{\partial x^2} \right) \frac{\partial N}{\partial t} - \left( \mu^2 \frac{\partial^2}{\partial t^2} - \gamma_0 \frac{\partial^2}{\partial x^2} - 1 \right) \frac{\partial M}{\partial x}, \end{aligned} \quad (23)$$

where  $\mathcal{L}$  is a linear operator and L is a function of the non-linear quantities P, N, and M. Similarly, with  $u_0$  we obtain:

$$\left[ \mu^2 \frac{d^2}{dt^2} + 1 \right] u_0 = T \quad (24)$$

Now we shall expand all dependent variables in terms of a small constant parameter  $\epsilon$ , in the following manner:

$$\left. \begin{aligned} v &= v^{(1)} \epsilon + v^{(2)} \epsilon^2 + v^{(3)} \epsilon^3 + \dots, \\ \gamma &= \gamma^{(1)} \epsilon + \gamma^{(2)} \epsilon^2 + \gamma^{(3)} \epsilon^3 + \dots, \end{aligned} \right\} \quad (25)$$

with similar expressions for the other quantities. Substituting these relations into equation (23), and equating the coefficients of like powers of  $\epsilon$ , we obtain the following system of linear equations:

$$\left. \begin{aligned} \mathcal{L}(v_T^{(1)}) &= 0, \\ \mathcal{L}(v_T^{(2)}) &= L_{11}, \\ \mathcal{L}(v_T^{(3)}) &= L_{12} + L_{21}, \\ \mathcal{L}(v_T^{(j)}) &= \sum_{k=1}^{j-1} L_{kj} v_T^{(k)}, \end{aligned} \right\} \quad (26)$$

where  $(uv)_{jR}$  means  $(u^{(j)} v^{(R)})$ . Notice that the first equation is homogeneous, and that the higher equations are inhomogeneous. Proceeding in a like manner with equation (24) yields:

$$\left. \begin{aligned} \left[ \mu^2 \frac{d^2}{dt^2} + 1 \right] u_0^{(1)} &= 0, \\ \left[ \mu^2 \frac{d^2}{dt^2} + 1 \right] u_0^{(j)} &= \sum_{k=1}^{j-1} T_{kj} u_0^{(k)}. \end{aligned} \right\} \quad (27)$$

These expansions must also be substituted into equations (16), (17), (18), (21), and (22). Now the system of equations may be solved by starting with the lowest order expressions, and an example of this procedure will be given in the next section.

#### Solution for a Particular Case

To solve the time dependent problem, the initial conditions must be specified. At this time we will not give these conditions exactly, but will indicate the general structure of the fields

initially. For very small disturbance amplitude, we require that the solution behave like the exponentially growing linear solution. Also, we desire that  $u_0, v_0$ , and  $\gamma$  be of smaller order than the other variables at this time.

The first step in the solution procedure is to obtain a solution to the equation

$$\mathcal{L}(v_T^{(1)}) = \left[ (\mu^2 \frac{\partial^2}{\partial t^2} - \gamma_0 \frac{\partial^2}{\partial x^2} + 1) \frac{\partial^2}{\partial t^2} - (\mu^2 \frac{\partial^2}{\partial t^2} - \gamma_0 \frac{\partial^2}{\partial x^2} - 1) \frac{\partial^2}{\partial x^2} \right] = 0. \quad (28)$$

For motions of period  $2\pi$  in  $X$  equation (28) has solutions of the form,  $Ae^{i(x+nt)}$ , where  $n$  satisfies the frequency equation:

$$\left[ (\mu^2 n^2 + \gamma_0 + 1)n^2 + (\mu^2 n^2 + \gamma_0 - 1) \right] = 0. \quad (29)$$

When  $\gamma_0$  is less than one, equation (29) has two real roots and two imaginary ones; the former correspond to baroclinic meteorological modes and the latter to gravitational-inertial modes.

We choose the solution of (28):

$$v_T^{(1)} = A \cos X e^{nt} \quad (30)$$

where  $\gamma_0 < 1$  and  $n$  is the real positive root of equation (29).

The corresponding solutions for the other field variables are:

$$v_m^{(1)} = \frac{A}{n} \sin X e^{nt} = D_{12} \sin X e^{nt} \quad (31)$$

$$u^{(1)} = -(n + \frac{1}{n}) A \cos X e^{nt} = C_{13} \cos X e^{nt} \quad (32)$$

$$\phi_T^{(1)} = [\mu^2(n^2+1)+1] A \sin X e^{nt} = D_{14} \sin X e^{nt}. \quad (33)$$

Also we will take zero solutions for  $u_0^{(1)}$ ,  $v_0^{(1)}$ , and  $\delta^{(1)}$ .

The initial amplitude for the first term in the series for  $v_T$  with this solution is  $\in A$ . In the higher order equations, we will take only the inhomogeneous part of the solution, so that the amplitude of each higher term in the series will contain  $\in A$  to the corresponding power. Thus, it is natural to take  $\in$  equal to the amplitude of the first term in the series for  $v_T$ , and this makes  $A$  equal to one.

To obtain the second term in the expansion, we must solve the equation:

$$\mathcal{L}(v_T^{(2)}) = L_{11} = \frac{\partial^2 P_{11}}{\partial x \partial t} + \left( \mu^2 \frac{\partial^2}{\partial t^2} - \gamma_0 \frac{\partial^2}{\partial x^2} \right) \frac{\partial N_{11}}{\partial t} - \left( \mu^2 \frac{\partial^2}{\partial t^2} - \gamma_0 \frac{\partial^2}{\partial x^2} - 1 \right) \frac{\partial M_{11}}{\partial x}. \quad (34)$$

In this case  $P_{11}$  vanishes since  $\delta^{(1)} = 0$ ,

$$N_{11} = -\mu \left[ u^{(1)} \frac{\partial v_m^{(1)}}{\partial x} - u^{(1)} \frac{\partial v_m^{(1)}}{\partial x} \right] = -\frac{\mu}{2} C_{13} D_{12} \cos 2x e^{2nt}, \quad (35)$$

and

$$M_{11} = -\mu \frac{\partial}{\partial x} (u^{(1)} v_T^{(1)}) = \mu C_{13} \sin 2x e^{2nt}, \quad (36)$$

where the  $C$ 's and  $D$ 's are defined in equations (31) through (34).

Substituting these relations into equation (34), we obtain the inhomogeneous solution:

$$v_T^{(2)} = -\frac{\mu C_{13}}{2} \frac{[2(\mu^2 n^2 + \gamma_0) n D_{12} + (\mu^2 4n^2 + 4\gamma_0 - 1)]}{(\mu^2 4n^2 + 4\gamma_0 + 1)n^2 + (\mu^2 4n^2 + 4\gamma_0 - 1)} \cos 2x e^{2nt} = C_{21} \cos 2x e^{2nt}, \quad (37)$$

where the homogeneous portion has been excluded. Also, the following solutions may be obtained for the other space dependent variables:

$$v_m^{(2)} = \frac{1}{2n} (2C_{21} + \mu C_{13}) \sin 2x e^{2nt} = D_{22} \sin 2x e^{2nt}, \quad (38)$$

$$u^{(2)} = (-2nC_{21} - 2D_{22} - \frac{\mu}{2} C_{13} D_{12}) \cos 2x e^{2nt} = C_{23} \cos 2x e^{2nt}, \quad (39)$$

$$\phi_T^{(2)} = (-n\mu^2 C_{23} + \frac{1}{2} C_{21}) \sin 2x e^{2nt} = D_{24} \sin 2x e^{2nt}. \quad (40)$$

It should be pointed out that the  $C$ 's and  $D$ 's employed above are functions only of  $\mu$  and  $\delta_0$ .

To obtain  $u_0^{(2)}$  we must solve the equation

$$\left[ \mu^2 \frac{d^2}{dt^2} + 1 \right] u_0^{(2)} = T_{11} = \mu \left( \frac{\partial u^{(1)}}{\partial x} v_m^{(1)} \right) = -\mu \frac{C_{13} D_{12}}{2} e^{2nt}. \quad (41)$$

The desired inhomogeneous solution is

$$u_0^{(2)} = -\frac{C_{13} D_{12}}{2(4n^2\mu^2 + 1)} e^{2nt} = J_2 e^{2nt}. \quad (42)$$

The other two dependent variables are given by:

$$v_0^{(2)} = 2n J_2 e^{2nt} \quad (43)$$

and

$$\gamma^{(2)} = \frac{\mu}{2n} (4n\mu J_2 - C_{13} D_{14}) e^{2nt} = E_2 e^{2nt}. \quad (44)$$

In a similar manner one may show that the third order solutions have the following form:

$$v_T^{(3)} = (C_{313} \cos 3X + C_{311} \cos X) e^{3nt}, \quad (45)$$

$$v_m^{(3)} = (D_{323} \sin 3X + D_{321} \sin X) e^{3nt}, \quad (46)$$

$$u^{(3)} = (C_{333} \cos 3X + C_{331} \cos X) e^{3nt}, \quad (47)$$

$$\phi_T^{(3)} = (D_{343} \sin 3X + D_{341} \sin X) e^{3nt}, \quad (48)$$

$$u_0^{(3)} = v_0^{(3)} = \gamma^{(3)} = 0. \quad (49)$$

Thus we see that our expansion is essentially a power series in  $e^{nt}$ , and for that reason it must diverge for sufficiently large  $t$ . Also it can be seen that a solution of order  $j$  will include spacial wave number  $j$  and possibly some longer waves. In the next section a physical discussion of the solutions will be given, when the above coefficients are computed for particular values of  $\mu$  and  $\gamma_0$ .

#### A Particular Example

The coefficients derived above are sufficiently complicated that it is difficult to study the solutions in general. Therefore, we will present the solutions for particular values of  $\mu$  and  $\gamma_0$  which are reasonable for large scale atmospheric flow. We choose  $\gamma_0 = .322$ , and  $\mu = .111$ , which correspond to  $U = 10.6$  meters per second,  $\frac{2\pi}{k} = 6 \times 10^6$  meters,  $-\frac{\partial \theta}{\partial p} = 5^\circ$  per 100 millibars, and  $f = 10^{-4} (\text{seconds})^{-1}$ .

We shall display the solutions in terms of  $v_1$  and  $v_3$ , instead of  $v_T$  and  $v_m$ , since the former quantities are the ones

observed on weather maps. The first three terms in the spatially varying part of  $v_1$  are:

$$v_1 - \bar{v}_1 = \epsilon e^{nt} [1.73 \sin(\chi + 35.4^\circ) - .96 \sin(2\chi - 53.3^\circ)(10^{-1} \epsilon e^{nt}) + (-.80 \sin(3\chi + 38^\circ) - 2.06 \sin(\chi + 86.5^\circ))(10^{-1} \epsilon e^{nt})^2 +], \quad (50)$$

where  $n = .712$ . Due to symmetry the  $v_3$  part of the solution will be of the same form, but the signs of the phase angles will be reversed. Notice that the expansion is in fact in powers of  $(10^{-1} \epsilon e^{nt})$ , which might be expected since the Rossby number is the coefficient of the non-linear terms which determine the higher order effects. Thus the series should converge for at least  $\epsilon e^{nt} = 1$ , and should diverge for  $\epsilon e^{nt} > 10$ . Equation (50) implies that the non-linear effects do not become very important until  $\epsilon e^{nt}$  exceeds 1, or 10 meters per second.

The first term in equation (50) represents the infinitesimal amplitude linear solution. The second term shows the growth of wave number two due to non-linear interaction. The distortion of the first order solution by the second is of such a form as to make the maximum north wind stronger than the maximum south wind, at the upper level. The distortion also gives sharper troughs and flatter ridges. Growing atmospheric disturbances often have these properties, although other explanations are possible. The third harmonic which appears in the third order expression is a distortion, which is created by the interaction of wave numbers one and two.

The other term in the third order expression represents the first feedback on wave number one, and is due to several physical effects. The contributions of the respective processes are:

$$\begin{aligned} & -1.69 \sin(\chi + 65^\circ) && \text{(static stability increase)} \\ & .82 \sin(\chi - 11.8^\circ) && \text{(mean zonal wind shear increase)} \\ & - .405 \sin(\chi + 67.5^\circ) && \text{(interaction between different wave} \\ & && \text{numbers)}. \end{aligned}$$

The static stability increase makes the largest contribution, and causes the overall growth rate of wave number one to be reduced. This behavior might be expected from the change in the linear growth criteria, due to an increase in the static stability. The zonal wind shear change causes wave number one to increase, which is reasonable since the linear growth rate is proportional to the zonal wind shear. Finally, the interaction between different wave numbers tends to decrease the amplitude of wave number one, since the amplitudes of the other waves are growing.

To be consistent with the above discussion the solution for  $\delta$  must give an increase in the static stability from the second order term. This is the case, and it should be expected since a vertical heat flux must accompany the energy conversion in the first order solution. Also, the first order solution has the proper form to give a vertical flux of  $\mathcal{V}$  momentum, which ultimately increases the mean zonal wind shear through the Coriolis force. This latter process is not thought to be important in the actual atmosphere

since the meridional circulation would reduce the poleward temperature gradient, and consequently the zonal wind shear.

#### Conclusion

The solutions obtained with this expansion technique, appear to be valid until the disturbances reach a substantial amplitude. The non-linear processes both distort the form of the infinitesimal amplitude solution, and modify its growth rate. The most important stabilizing influence arises from the time variation of the static stability. The solutions also indicate an energy cascade, which could not occur in a quasigeostrophic model with no  $y$  variation.

A more complete discussion of the physical processes should be given, with special emphasis on the energetics. Some indication of the effect of two horizontal dimensions is needed, and might be obtained from a similar expansion. These studies could be generalized by allowing  $f$  and the static stability to vary in the horizontal. Also, heating and friction might be included, and steady state solutions sought. However, in considering the desirability of such extensions, the increased complexity in the procedure must be kept in mind.

#### Acknowledgments

The author wishes to thank Dr. M. Stern and Prof. W.V.R. Malkus for many useful discussions, and the NSF for supporting his participation in the program.

References

- Eliassen, A., 1956: A procedure for numerical integration of the primitive equations of the two-parameter model of the atmosphere. University of California at Los Angeles, Dept. of Meteorology, Large Scale Synoptic Processes Project, Scientific Report No. 4, 53 pp.
- Hinkelmann, K., 1959: Ein numerisches experiment mit den primitiven gleichungen. The Atmosphere and the Sea in Motion, (edited by B. Bolin), Rockefeller Institute Press in association with the Oxford University Press, New York, pp.486-500.
- Malkus, W.V.R. and G. Veronis, 1958: Finite amplitude cellular convection. J.Fluid Mech., 4, pp.225-260.
- Phillips, N.A., 1959: An example of non-linear computational instability. The Atmosphere and the Sea in Motion, (edited by B. Bolin), Rockefeller Institute Press in association with the Oxford University Press, New York, pp.501-504.
- Smagorinsky, J., 1958: On the numerical integration of the primitive equations of motion for baroclinic flow in a closed region. Monthly Weather Review, 86, pp.457-466.